8-16-2013

A revised 1000 year atmospheric δ^{13} C-CO2 record from Law Dome and South Pole, Antarctica

M. Rubino
CSIRO Marine and Atmospheric Research

D. M. Etheridge
CSIRO Marine and Atmospheric Research

C. M. Trudinger
CSIRO Marine and Atmospheric Research

C. E. Allison
CSIRO Marine and Atmospheric Research

M. O. Battle
Bowdoin College

See next page for additional authors

A revised 1000 year atmospheric ^{13}C-CO_2 record from Law Dome and South Pole, Antarctica

M. Rubino,[1,2] D. M. Etheridge,[1,2] C. M. Trudinger,[1] C. E. Allison,[1] M. O. Battle,[3] R. L. Langenfelds,[1] L. P. Steele,[1] M. Curran,[4] M. Bender,[5] J. W. C. White,[6] T. M. Jenk,[2] T. Blunier,[2] and R. J. Francey[1]

Received 19 February 2013; revised 19 June 2013; accepted 16 July 2013; published 15 August 2013.

[1] We present new measurements of $\delta^{13}C$ of CO_2 extracted from a high-resolution ice core from Law Dome (East Antarctica), together with firn measurements performed at Law Dome and South Pole, covering the last 150 years. Our analysis is motivated by the need to better understand the role and feedback of the carbon (C) cycle in climate change, by advances in measurement methods, and by apparent anomalies when comparing ice core and firn air $\delta^{13}C$ records from Law Dome and South Pole. We demonstrate improved consistency between Law Dome ice, South Pole firn, and the Cape Grim (Tasmania) atmospheric $\delta^{13}C$ data, providing evidence that our new record reliably extends direct atmospheric measurements back in time. We also show a revised version of early $\delta^{13}C$ measurements covering the last 1000 years, with a mean preindustrial level of –6.50 . Finally, we use a Kalman Filter Double Deconvolution to infer net natural CO_2 fluxes between atmosphere, ocean, and land, which cause small $\delta^{13}C$ deviations from the predominant anthropogenically induced $\delta^{13}C$ decrease. The main features found from the previous $\delta^{13}C$ record are confirmed, including the ocean as the dominant cause for the 1940 A.D. CO_2 leveling. Our new record provides a solid basis for future investigation of the causes of decadal to centennial variations of the preindustrial atmospheric CO_2 concentration. Those causes are of potential significance for predicting future CO_2 levels and when attempting atmospheric verification of recent and future global carbon emission mitigation measures through Coupled Climate Carbon Cycle Models.

Citation: Rubino, M., et al. (2013), A revised 1000 year atmospheric $\delta^{13}C$-CO_2 record from Law Dome and South Pole, Antarctica, *J. Geophys. Res. Atmos.*, *118*, 8482–8499, doi:10.1002/jgrd.50668.

1. Introduction

[2] Attributing causes to past variations of atmospheric carbon dioxide (CO_2) concentration (defined as the mole fraction of CO_2 in dry air) will help to improve prediction of the future interplay between the climate and the carbon cycle. Studies of CO_2 and its $^{13}C/^{12}C$ stable isotope ratio (referred to as $\delta^{13}C$ from here on), involving overlapping Antarctic ice cores, firn and contemporary air records, remain key evidence for recent natural variations in the C cycle as well as the impact of human CO_2 emissions on the global atmosphere.

[3] The record of atmospheric CO_2 concentration extracted from the ice cores drilled at Law Dome (East Antarctica) covering the last 2000 years [*Etheridge et al.*, 1996; *MacFarling Meure et al.*, 2006] has been extensively used in modeling studies to constrain the global C cycle of the past [*Joos and Bruno*, 1998; *Trudinger et al.*, 1999, 2005] and its interactions with the climate system [*Ammann et al.*, 2007; *Cox and Jones*, 2008; *Frank et al.*, 2010]. Models of the global C cycle that include the stable isotopes of C [*Joos et al.*, 1999; *Trudinger et al.*, 2002b; *Gerber et al.*, 2003; *Köhler et al.*, 2006] have found an additional constraint in the companion record of $\delta^{13}C$ from the same site in Antarctica [*Francey et al.*, 1999, hereinafter F99]. This is a high precision data set, due to meticulous examination of all aspects of the procedure, representing the state of the art in 1999 for measured $\delta^{13}C$ changes in air trapped in ice cores. The Law Dome $\delta^{13}C$ record has shown late preindustrial

Additional supporting information may be found in the online version of this article.

[1]Center for Australian Weather and Climate Research, CSIRO Marine and Atmospheric Research, Aspendale, Victoria, Australia.
[2]Center for Ice and Climate, Niels Bohr Institute, University of Copenhagen, Copenhagen, Denmark.
[3]Department of Physics and Astronomy, Bowdoin College, Brunswick, Maine, USA.
[4]Department of the Environment and Heritage, Australian Antarctic Division, Antarctic Climate and Ecosystem Cooperative Research Center, Hobart, Tasmania, Australia.
[5]Department of Geosciences, Princeton University, Princeton, New Jersey, USA.
[6]Institute of Arctic and Alpine Research, University of Colorado Boulder, Boulder, Colorado, USA.

Corresponding author: M. Rubino, Center for Australian Weather and Climate Research, CSIRO Marine and Atmospheric Research, 107-121 Station Street, Aspendale, Vic 3195, Australia. (mauro.rubino@csiro.au)

2169-897X/13/10.1002/jgrd.50668

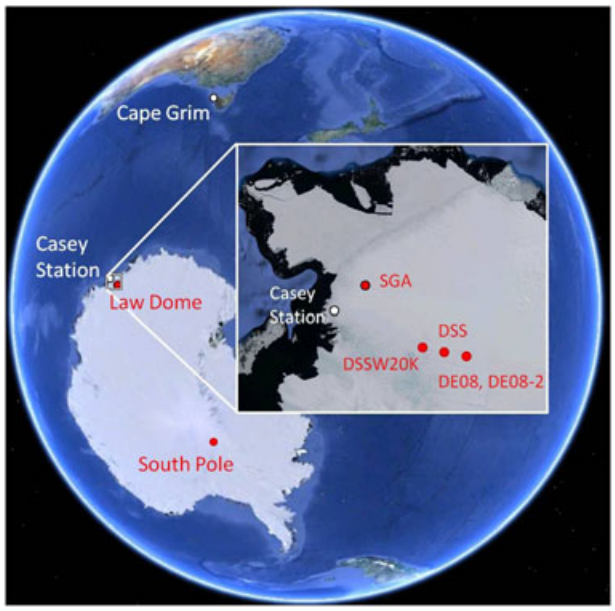

Figure 1. Approximate locations of the ice core drilling sites (Law Dome), firn (Law Dome and South Pole), and atmospheric (Cape Grim) sampling sites used in this study. Names in red correspond to ice core drilling and firn sampling sites; names in white correspond to atmospheric sampling stations. The location of Casey station is given as a reference, but data from Casey station have not been used in this study.

Holocene (LPIH) variations of atmospheric δ^{13}C and has confirmed that the CO_2 released into the atmosphere during the Industrial Period, since 1750 A.D.) has a C source depleted in ^{13}C, providing key evidence for the attribution of atmospheric CO_2 variations during the Industrial Period to anthropogenic activities.

[4] Thanks to the characteristics of the drilling sites at Law Dome (high accumulation rate, low temperature, and small quantities of impurities in the ice) [*Etheridge and Wookey*, 1989; *Morgan et al.*, 1997], no other ice core has, so far, provided such a precise and well-resolved δ^{13}C record of the last 1000 years. Even though another high-resolution record of δ^{13}C over the Industrial Period was produced by *Kawamura et al.* [2000] from the Antarctic H15 ice core, unexplained differences from the F99 data set of, on average, 0.2–0.3 in the mean level and up to 0.5 around 1800 A.D. were found. Records of δ^{13}C covering the last glacial period [*Machida et al.*, 1996; *Smith et al.*, 1999] or the Holocene period [*Indermühle et al.*, 1999; *Elsig et al.*, 2009] do not both span the LPIH and overlap firn measurements and have used the F99 record to link their longer records to direct atmospheric measurements. No other paleoarchives (speleothems, corals, and sediments) have been found to be comparably useful, especially in the Industrial Period.

[5] More than 10 years after its publication, the Law Dome δ^{13}C record remains one of the main sources of information for models inferring the C sources and sinks associated with past variations of atmospheric CO_2 concentration over the last 1000 years [*Stocker et al.*, 2011]. Nevertheless, the sampling density of the Law Dome δ^{13}C record needs to be increased, especially over the LPIH where significant changes of the atmospheric CO_2 concentration have been found (e.g., beginning of the seventeenth century) [*MacFarling Meure et al.*, 2006]. This can improve our understanding of the mechanisms responsible for natural changes of the atmospheric CO_2 concentration in a period, like the LPIH, where the Earth's system was very close to current conditions, but with anthropogenic influences not yet a predominant part of the carbon cycle.

[6] Measurements of δ^{13}C in air extracted from the firn have been used to match the F99 record with modern atmospheric measurements. The firn is the upper part of an ice sheet, where bubbles are not yet closed, and air with mean age up to several decades can be pumped directly out of the snow matrix and collected for analysis [*Schwander et al.*, 1988]. Shallow firn air measurements can be compared to direct atmospheric measurements of δ^{13}C [*Sugawara et al.*, 2003; F99], which started in 1976 at Mauna Loa in the Northern Hemisphere [*Keeling et al.*, 1989] and in 1978 at Cape Grim in the Southern Hemisphere [*Allison and Francey*, 2007]. Similarly, deep firn air measurements can be compared to ice core data. While recent (younger than 1950 A.D.) ice core air samples from Law Dome agreed closely with Law Dome firn air and direct atmospheric records, a difference with older South Pole firn samples became apparent [*Trudinger*, 2000, p. 108].

[7] This study follows and further develops the experience gained from the F99 study, where it was stated that "a number of opportunities to improve precision have been identified, including the more accurate determination of the relative gravitational corrections between ice cores, and cores versus firn ... and reduced sensitivity to blank and sample size biases." We present new measurements of δ^{13}C from ice and firn air covering the last 150 years, together with a revision of the δ^{13}C record from F99. Measurements of multiple species (CO_2, δ^{13}C, δ^{18}O, CH_4, CO, and N_2O) allow independent verification of sample quality, corrections for mass spectrometry, and insight into biogeochemical processes. We show how a slightly modified method for extracting and measuring air from bubbles in ice, combined with more consistent and strict criteria of sample and measurement selection, has allowed us to resolve the discrepancy found in the past between Law Dome ice and South Pole firn air. Finally, we show the attribution of sources and sinks of atmospheric CO_2 identified through a Kalman filter double deconvolution (KFDD) [*Trudinger et al.*, 2002b] of this revised record.

2. Materials and Methods

2.1. Ice, Firn, and Atmospheric Samples

[8] The ice and firn samples used in this study were collected from two different locations in Antarctica (East Antarctica and South Pole, Figure 1).

[9] Measurements of δ^{13}C from those sites will be compared to the atmospheric Cape Grim (40 41′0″S, 144 41′42″E, Figure 1) δ^{13}C record, which has provided an uninterrupted baseline δ^{13}C record in the Southern Hemisphere since the beginning of the 1980s [*Allison and Francey*, 2007], with improved traceability after 1992. Attributing the δ^{13}C latitudinal gradient observed between Tasmania and the coast of Antarctica on a number of

Table 1. Details of the Ice Core and Firn Sampling Sites Used in This Study[a]

Site Code	Sampling Type	Location	Sampling Date (A.D.)	Depth[b] Range (m)	Mean Temperature (C)	Accumulation Rate (kg m^{-2} yr^{-1})	CO_2 Age[b] Range (A.D.)	Spectral[c] Width (year)
DE08	Ice	66 43′S, 113 12′E	1987	79–234	–19	1100	1843–1972	4.5 (4.4–4.7)
DE08-2	Ice	66 43′S, 113 12′E	1993	85–234	–19	1100	1833–1974	4.5 (4.4–4.7)
DSS	Ice	66 46′S, 112 48′E	1988–1993	78–772	–22	600	1019–1962	5.8 (3.7–7.8)
DE08-2	Firn	66 43′S, 113 12′E	1993	0–85	–19	1100	1976–1993	
SPO1995	Firn	90 S	1995	0–122	–49	75	1897–1995	16.0 (15.7–18.9)
DSSW20K	Firn	66 46′S, 112 21′E	1997	0–52	–20.7	150	1938–1996	7.0 (6.5–8.5)
SPO2001	Firn	90 S	2001	0–119.9	–49	75	1929–2001	18.1 (17.2–18.2)

[a]Site codes follow the names used in the text (SPO stands for South Pole). CO_2 age range refers to the selected samples shown in Figures 4 and 5.
[b]Depth and CO_2 age ranges refer to the samples used in this study.
[c]Spectral width refers to CO_2 dated 1940 A.D. firn for all but DE08 and DE08-2. Numbers in parentheses are model estimated 1σ ranges (see section 2.4).

(mainly summer) ship transects [*Beggs*, 1996] to an ocean-atmosphere ^{13}C disequilibrium flux due to the temperature dependence of the air-sea fractionation factor [*Mook et al.*, 1974], F99 adjusted the Cape Grim data by 0.015 for comparison with Antarctic firn; for consistency, we use the same adjustment here.

2.1.1. Law Dome Ice

[10] The ice cores used in this study, referred to as DE08, DE08-2, and DSS, were drilled at Law Dome, East Antarctica (see Figure 1 and Table 1 for the site location and characteristics). DE08 and DE08-2 were drilled in 1987 and 1993, respectively, only 300 m apart and 16 km east of the summit (66 44′S, 112 50′E, 1390 m above mean annual sea level), and have an accumulation rate of approximately 1.4 m ice equivalent per year. DSS (Dome Summit South) was drilled between 1988 and 1993, 4.6 km south-southwest of the summit, and has an accumulation rate of about 0.7 m ice equivalent per year. For more information about the characteristics of the Law Dome site and those of the ice cores, see *Goodwin* [1990] and *Etheridge et al.* [1996], respectively.

2.1.2. Firn Sampling

[11] Firn air samples were taken using the procedure described in *Etheridge et al.* [1996]. Briefly, firn air was sampled by lowering a Firn Air Sampling Device, consisting of an inflatable bladder with several air lines passing through, to the bottom of the ice core borehole at each desired depth. The bladder sealed the borehole, and air samples were drawn from the firn layer below and collected in glass flasks and stainless steel containers. The procedure was repeated until impermeable ice was reached at the bottom of the firn column. Ambient air samples collected using the same procedure, but with the Firn Air Sampling Device inlet on the snow surface confirmed no influence of the Firn Air Sampling Device on the composition of the sampled air.

[12] In January-February 1993, air was sampled from the firn layer at DE08-2, providing air as old as 1976 A.D. [*Etheridge et al.*, 1996]. Another firn campaign was carried out at DSSW20K (accumulation rate of approximately 0.17 m ice equivalent per year), 20 km west of DSS (Figure 1) in December 1997 [*Sturrock et al.*, 2002]. These conditions provided air dated back to ~1940 A.D. [*Trudinger et al.*, 2002a]. During the DSSW20K sampling campaign, firn air was also sampled from other sites including SGA (Strain Grid A, Cape Folger region, Figure 1), and because no surface sample had been collected at DSSW20K, we rely on the surface sample collected at SGA to show that no significant influence of the Firn Air Sampling Device on the composition of the sampled air was found during the 1997 firn campaign.

[13] Firn air was collected at the South Pole in January 1995 and in January 2001 [*Battle et al.*, 1996; *Butler et al.*, 2001]. South Pole is an extremely cold site (see Table 1), with a very low accumulation rate (approximately 8 cm ice equivalent per year) [*Gow*, 1965]. This leads to the deepest known firn-ice transition of ~123 m (the depth where it is no longer possible to pump air out of the firn), which preserves particularly old air at the base of the firn column, though with a very broad age spread (see section 2.4). During the South Pole campaigns, samples were collected from pairs of boreholes following the protocols described by *Battle et al.* [1996]. The only substantive difference in the sampling equipment between these two campaigns was a change in the tubing through which the samples were collected (from nylon to Synflex, also known as Dekabon or Dekoron).

2.2. Experimental Procedure

[14] Here we use the δ notation to report the stable carbon and oxygen isotopic composition of CO_2 (δ^{13}C and δ^{18}O) as:

$$\delta^{13}\mathrm{C} = \left[\frac{r^{13}_{sa}}{r^{13}_{st}} - 1\right] 1000 \quad \delta^{18}\mathrm{O} = \left[\frac{r^{18}_{sa}}{r^{18}_{st}} - 1\right] 1000 \qquad (1)$$

where r^{13} is the ratio of heavy carbon isotope (^{13}C) to the light isotope (^{12}C), r^{18} is the ratio of heavy oxygen isotope (^{18}O) to the light isotope (^{16}O), and the subscripts sa and st refer to the ratios in the sample and standard gas, respectively.

[15] For the corrections discussed in the following sections, it is worth specifying that conventional isotope ratio mass spectrometers (IRMS) do not measure the δ^{13}C and δ^{18}O of CO_2 directly, rather the ion currents, i^m, are measured at the mass-to-charge ratios of m/z = 44 ($^{12}C^{16}O^{16}O$), m/z = 45 ($^{13}C^{16}O^{16}O$ and $^{12}C^{16}O^{17}O$), and m/z = 46 ($^{12}C^{16}O^{18}O$, $^{12}C^{17}O^{17}O$, and $^{13}C^{16}O^{17}O$). In this study, the ion current ratios, r^{45} (= i^{45}/i^{44}) and r^{46} (= i^{46}/i^{44}), are calculated for both the sample and reference CO_2 over eight alternating integrations (from now on referred to as

acquisitions), and the difference between these two ratios is reported as a δ^m value, where $m = 45$ or 46.

$$\delta^m = \left[\frac{r^m_{sa}}{r^m_{st}} - 1 \right] 1000 \quad (2)$$

[16] These $\delta^{45}CO_2$ and $\delta^{46}CO_2$ measurements are then converted to $\delta^{13}C$ and $\delta^{18}O$ values in the sample CO_2 and reported relative to those in the international reference Vienna Peedee belemnite (VPDB), as described in *Allison and Francey* [2007], with a revised ion correction procedure [*Brand et al.*, 2010].

2.2.1. Firn Measurements

[17] All the Law Dome firn samples and six samples from two levels from the South Pole 2001 firn campaign (corresponding to the surface and the deepest layer at 119.87 m depth) were measured in the Global Atmospheric Sampling Laboratory (GASLAB) at the Commonwealth Scientific and Industrial Research Organisation (CSIRO; Division of Marine and Atmospheric Research) in Aspendale, Victoria (Australia), according to the procedures developed for the analysis of trace gases concentration (CO_2, CH_4, CO, H_2, and N_2O) and the stable isotope ratios $\delta^{13}C$ and $\delta^{18}O$ of CO_2 [*Francey et al.*, 1996] of atmospheric samples.

[18] Measurements of CO_2 and N_2O concentration on the firn air samples collected at the South Pole in 1995 [*Battle et al.*, 1996] and 2001 [*Butler et al.*, 2001] were performed at the National Oceanic and Atmospheric Administration/Climate Modeling and Diagnostics Laboratory (NOAA/CMDL). Measurements of $\delta^{13}C$ on the firn air samples collected at South Pole in 1995 were performed in GASLAB, whereas those for South Pole firn collected in 2001 were performed at the Institute of Arctic and Alpine Research (INSTAAR). An ongoing $\delta^{13}C$ calibration scale comparison between CSIRO and INSTAAR, based on 20 years of flask analysis from the Cape Grim flask program [*Masarie et al.*, 2001], has allowed us to estimate the relevant offset between the two laboratories.

2.2.2. Extraction of Air From Ice Bubbles

[19] Ice samples require an extraction step to release the air sample from ice bubbles and remove water from it. The extraction of air from ice uses a dry grating technique in the Ice Core Extraction Laboratory (ICELAB) at the CSIRO in Aspendale [*Etheridge et al.*, 1988]. Briefly, after sample selection and preparation (removing the outer 5–20 mm with a band saw), typically 0.7–1.3 kg of ice was placed in a polyethylene bag (Layflat, USP®) and cooled down to –80 C in a chest freezer for at least 24 h prior to extraction. The ice was then sealed in an internally electropolished stainless steel container containing a perforated inner cylinder (referred to as the cheese grater) [*Etheridge et al.*, 1996] and the vessel evacuated to less than 10^{-4} Torr for at least 25 min. The ice was grated by mechanically shaking the container for 10 min. This process yielded on average 70 mL (range 50–90 mL) of air, estimated by the pressure in the extraction line (whose volume had been previously calibrated). The air was cryogenically collected in an electropolished and preconditioned stainless steel trap at around 23–24 K, after removing water at –100 C. The sample trap was warmed in a water bath at room temperature for 5 min and analyzed on the Gas Chromatographs (GCs) for CO_2, CH_4, CO, H_2, and N_2O within 1 h from extraction and on the IRMS for $\delta^{13}C$ and $\delta^{18}O$ within 12 h.

[20] The extraction and measurement procedures, described in *Etheridge et al.* [1996] and F99, respectively, were adapted or slightly modified to decrease the extraction time and optimize the $\delta^{13}C$ analysis:

[21] 1. Three ice grating containers, numbered 1, 6, and 7, with different geometries and sealed with different materials, were tested to improve crushing efficiency, vacuum performance, and ease of assembly (the characteristics of the three graters are described in section A1).

[22] 2. Each air sample was measured as soon as possible after extraction (typically within 1 h on the GCs and 12 h on the IRMS), thereby minimizing unwanted storage effects, such as the isotopic effects on $\delta^{46}CO_2$ described in section 3.1;

[23] 3. The water trap at –100 C was regenerated after every extraction to maximize the trapping efficiency;

[24] 4. The indium wire used to seal grater 1 was replaced daily, after every fourth extraction, and the grater was disassembled and washed in 3% solution of NEUTRACON (Decon Laboratories Limited, East Sussex, UK) in water, rinsed twice with tap water and twice with deionized water, baked at 120 C for 72 h and "steam cleaned" at 120 C for 24 h with a 4 L min^{-1} flow of deionized water-saturated air;

[25] 5. The volume of the vacuum line was determined to allow the extracted air volume to be estimated from the pressure measurement, thus enabling more efficient use of the extracted sample.

[26] The results of the tests listed at steps 1–5 will be discussed in section 3.1.

[27] In order to quantify the uncertainty associated with each step of the gas extraction procedure, we cryogenically collected air of known composition from the grater while varying the factors that were believed to influence the precision of our procedure: with/without shaking the grater, with/without ice releasing water vapor in the grater. We used a high-pressure cylinder of natural air filled in September 1996 at Cape Schanck (38.5 S 144.9 E) in conditions of strong winds from the south-west (Southern Ocean) sector, diluted with air-containing zero concentration of trace gases to simulate preindustrial CO_2 concentrations (i.e., 284.2 ppm, with $[CH_4]$ = 1281.8 ppb, [CO] = 70.3 ppb, $[N_2O]$ = 237.4 ppb, $\delta^{13}C$ = –7.82 , and $\delta^{18}O$ = –5.82).

[28] The methods to estimate the total analytical uncertainty and the results obtained will be described in section 3.1.

2.2.3. GC and IRMS Analyses of Air Extracted From Ice

[29] Each extracted air sample was analyzed for trace gas concentrations using GCs in GASLAB following the procedure [*Etheridge et al.*, 1988; *Francey et al.*, 1996] summarized in section A2. The $\delta^{13}C$ and $\delta^{18}O$ of the CO_2 in the residual air was measured using the IRMS (MAT252, Finnigan) located in GASLAB [*Allison and Francey*, 2007]. The IRMS uses a cryogenic trapping procedure (MT Box C, Finnigan) to extract CO_2 from air.

2.2.3.1. Methodological Differences From the F99 Study

[30] The stable isotope measurements and calibration procedures have some significant differences from those used in the F99 study, and some of them are described in *Allison and*

Francey [2007] (see also section A3 for details on recent calibration scale changes). Besides changes in the CSIRO $\delta^{13}C$ calibration scale, the following modifications to the methods used in the F99 study are significant in the present study:

[31] 1. Installation of a mass flow controller has improved trapping reproducibility, due to better control of the rate of CO_2 extraction from the air sample. For ice core samples, where the volume of air is variable and the entire sample is processed, this means that the pressure in the cryogenic traps of the MT Box C is constant and consistent, for all samples, whereas previously, it varied with sample size and decreased quickly during the trapping procedure. Thus, the sample size correction applied in F99, depending on the voltage measured on the Faraday cups of the IRMS and introducing a variable change of the measured $\delta^{45}CO_2$ (–0.01 to 0.07) and $\delta^{46}CO_2$ (–1.4 to 0.4), was unnecessary. By using the estimates of sample size determined during extraction of air from ice (see point "e" in section 2.2.2), we were able to introduce aliquots of standard gas that yielded matching sample and standard signals (sample to standard voltage ratio as close to 1 as possible), obviating the correction.

[32] 2. The isotopic enrichment occurring within the IRMS reference gas reservoir during analysis as the CO_2 is removed via a capillary (the so-called bleed correction, which causes a very small change of less than 0.02 in $\delta^{45}CO_2$ and less than 0.04 in $\delta^{46}CO_2$) has been better quantified [*Allison and Francey*, 2007].

[33] 3. Artifacts associated with the sample/reference mixing (the cross contamination, see section A4) in the MAT252 have been estimated and corrected for. This correction removes a variability that is in the range –0.06 to 0.06 for $\delta^{45}CO_2$ and about double (–0.12 to 0.12) for $\delta^{46}CO_2$.

[34] 4. A new ^{17}O-correction algorithm [*Brand et al.*, 2010] has been used to derive $\delta^{13}C$ and $\delta^{18}O$ from the measured $\delta^{45}CO_2$ and $\delta^{46}CO_2$ allowing improved external comparisons (with other data sets). The impact on all measured $\delta^{13}C$ is small, less than 0.05 , and it is applied consistently over all measurements, present and past.

[35] 5. All samples were analyzed in a sequence that involved bracketing measurements of well-characterized air standards to simulate the measurement of a sample and correct for any measured bias.

[36] All the mentioned effects accounted for, on average, 0.07 difference between the revised ice core $\delta^{13}C$ measurements and those from the F99 study. We will show in section 3.2 that the rest of the difference (about 0.1 , giving a total difference of, on average, –0.17 , with the revised data set more negative than the previous one) is associated with the correction applied to take into account the systematic effects measured during extraction of air from ice.

2.3. Firn Model

[37] We used the CSIRO firn model [*Trudinger et al.*, 1997, 2013] to date firn air and provide corrections for gravity and diffusion fractionation. For each site, we specify mean annual temperature, pressure, accumulation rate, the depth profile of firn density, profiles of closed and open porosity versus density, and we calibrate effective diffusivity (or, more accurately, inverse tortuosity) versus porosity to give optimum agreement between modeled and measured concentrations of tracers. All details of sites used here (except DSS) are given in *Trudinger et al.* [2013]. For DSS, there are no measurements of firn air to tune the firn model diffusivity, and no closed porosity measurements. Therefore, we used the empirical fit to DSS density measurements, described in *van Ommen et al.* [1999], with five different closed porosity profiles based on measurements for DE08-2 and an ensemble of diffusivity profiles calibrated to DE08-2 firn measurements. We selected as our best case for DSS the diffusivity profile that best matched the measured $\Delta^{14}C$-CO_2 bomb pulse in DSS ice [*Smith et al.*, 2000].

[38] We can quantify the age distribution at each site by the spectral width (see Table 1), analogous to the standard deviation for nonsymmetrical age distribution [*Trudinger et al.*, 2002a]. In order to reflect uncertainties in the firn model, calculations were performed with an ensemble of diffusivity parameters, all of which gave a good fit to the tuning observations [*Trudinger et al.*, 2013].

[39] We have also employed a different, but closely related, firn model to test the robustness of the inferred atmospheric $\delta^{13}C$ history. This model, developed at the Bowdoin College, has been successfully employed in other studies [*Mischler et al.*, 2009; *Battle et al.*, 2011], and, in this study, was used to produce a $\delta^{13}C$ versus depth firn profile for South Pole 2001 firn and compare it to the $\delta^{13}C$ firn profile measured at INSTAAR. There are three versions of the Bowdoin firn model, but the version used in this study is conceptually equivalent to the CSIRO model.

2.4. Air Dating

[40] Diffusive mixing within the firn column and gradual bubble close off cause the air at any depth to be younger than the ice at the same depth, and to have an age spread. Therefore, assigning an age to each air sample extracted from ice and firn is not trivial and requires several steps.

[41] Dating firn air is best done with a firn model when the model can be constrained by measurements of firn gases with known atmospheric histories. To date the age of air in the trapped bubbles, the age of ice needs to be assigned, and then, the age of air in ice is related to the age of the ice, with a gas-age/ice-age difference.

[42] DE08 and DE08-2 ice was dated by counting the annual layers in oxygen isotope ratio ($\delta^{18}O$-H_2O), ice electroconductivity, and hydrogen peroxide (H_2O_2) and checking against independently dated volcanic horizons [*Etheridge et al.*, 1996]. The ice dating for DE08 and DE08-2 was recently checked with additional, seasonally varying chemistry measurements and found to agree within 2 years back to 1815 (the year of eruption of Mount Tambora in Indonesia).

[43] The firn model, with measured closed porosity and with diffusivity calibrated to DE08-2 firn concentration, gives a gas-age/ice-age difference of 31 years for CO_2. This was used here for DE08 and DE08-2 and is in agreement (within 1 year) with the previous result from consideration of the density profile and age of ice at close off [*Etheridge et al.*, 1996; *Levchenko et al.*, 1996]. For ice samples below the firn to ice transition, an additional spread in air age is due to the bubbles that close off at different times above the sealing depth. However, for DE08 and DE08-2, no significant additional spread is introduced when the firn model is run to estimate the age distribution in ice because the very

high accumulation rate causes bubble close off to occur over a very short time span.

[44] Being deeper than DE08, DSS ice is more difficult to date, requiring inputs from ice flow models. The previously used DSS ice core age scale (LD1) [*van Ommen et al.*, 2004] has been recently updated [*Plummer et al.*, 2012] and shows a difference of less than 2 years from LD1 back to year 1000 A.D. The model estimated gas-age/ice-age difference for DSS is 54.8 years for our best case, with a range of 52.7–59.3 years from an ensemble of model parameters. The previously estimated gas-age/ice-age difference for CO_2 was 61 years [*Etheridge et al.*, 1996]. Since the firn model is not well constrained at DSS, we have no compelling reason to prefer the best model value over the previous one. This last number has been adopted in this study because it is consistent with previous work [*MacFarling Meure et al.*, 2006] and provides the age for which measurements of CH_4 concentration in DSS ice best overlap the measured CH_4 at DE08 and DE08-2 ice and the age which is more consistent with the measured Δ^{14}C-CO_2 bomb pulse [*Smith et al.*, 2000].

2.5. Kalman Filter Double Deconvolution

[45] A double deconvolution [*Keeling et al.*, 1989; *Francey et al.*, 1995; *Joos et al.*, 1999] uses CO_2 and δ^{13}C to estimate the net fluxes of CO_2 between the atmosphere and terrestrial biosphere and the atmosphere and oceans. We use the KFDD from *Trudinger et al.* [2002b], which combines statistical analysis and a carbon cycle model, allowing estimation of uncertainties in the fluxes. The KFDD is well suited for interpretation of ice core data with long gaps. Unlike the mass balance double deconvolution based on spline fits to the observations [*Joos and Bruno*, 1998], the KFDD does not assume values for either CO_2 or δ^{13}C in the data gaps, leading to more rigorous uncertainty analysis. A (globally aggregated) carbon cycle model is needed in the double deconvolution to calculate the isotopic disequilibrium fluxes, and for this, we use the box diffusion model mixed layer pulse response function from *Joos et al.* [1996] and the two-box terrestrial biosphere model from *Trudinger et al.* [1999]. Parameters in the biosphere model were chosen so that our calculation gives recent terrestrial and ocean net fluxes similar to those estimated by GCP 2010 (Global Carbon Project budget at http://www.tyndall.ac.uk/global-carbon-budget-2010). Here we are interested in decadal variations in fluxes over the Industrial Period and century-scale variations back to 1000 A.D.

[46] The measurements we use are the firn and ice core measurements presented in this paper (except South Pole), as well as annual mean values of CO_2 and δ^{13}C at Cape Grim from 1992 [*Allison and Francey*, 2007]. We correct these Southern Hemisphere measurements to reflect global levels using

$$\text{global} = \text{SH} - 0.4 + 2.4 \times \frac{\text{foss}}{8.0} \tag{3}$$

for CO_2 and

$$\text{global} = \text{SH} - 0.06 \times \frac{\text{foss}}{8.5} \tag{4}$$

for δ^{13}C, where SH is the CO_2 or δ^{13}C measured at Antarctica or Cape Grim. This assumes a LPIH CO_2 gradient of 0.4 ppm in the opposite sense to today's gradient, and no LPIH gradient in δ^{13}C, and a modern difference in Southern Hemisphere CO_2 and δ^{13}C from global of 2.4 ppm and –0.06 , respectively, and uses fossil fuel emissions (foss) to interpolate between these values [*Conway and Tans*, 1999]. There is some uncertainty in these values, but they are not particularly important for our KFDD as we are mainly interested in decadal and century-scale variations (rather than the industrial perturbation). We specify global fossil fuel emissions [*Boden et al.*, 2011], land use change (*Houghton* [2008] before 1958 and GCP 2010 after), and δ^{13}C of the fossil fuel emissions [*Andres et al.*, 2011].

[47] The KFDD needs observation errors and the covariance of stochastic forcing (**Q**, which describes how much the net fluxes can change from year to year) to be specified and uses the chi-squared test to ensure consistent values [*Trudinger et al.*, 2002b]. We use the observation errors from this work, but based on variations in samples with similar ages and confirmed by a chi-squared test, we impose a lower bound of 1.2 ppm for CO_2 and 0.05 for δ^{13}C (see section 3.1.3). For **Q**, for both land and ocean fluxes, we use 0.01 (GtC yr^{-1})^2 for the LPIH (chosen to highlight century timescales due to the data density) and 0.1 (GtC yr^{-1})^2 for the Industrial Period (reflecting variability that survives firn diffusion and bubble trapping at DE08 and DE08-2) [*Trudinger et al.*, 2002b].

[48] We excluded the South Pole firn data from the double deconvolution calculation because the spectral width varies with depth, and in the deep firn, it is significantly larger than at the Law Dome sites (Table 1). To use the South Pole data in the deconvolution, we should take into account this variation in spectral width with depth (such as by the use of different age distributions for different measurements). By using mainly DE08 and DE08-2 ice core measurements that have constant age distributions, as well as a few DSSW20K firn measurements with spectral widths that are not significantly different to that for DE08, we can avoid this issue and take into account firn processes through our choice of **Q**.

2.6. Corrections for Gravitational and Diffusion Fractionation

2.6.1. Gravity Correction

[49] Gravitational enrichment of heavier species in air in the firn open porosity [*Craig et al.*, 1988; *Schwander*, 1989] causes the CO_2 concentration and δ^{13}C measured in firn and ice to be higher (more positive) than the original atmospheric values, and needs to be taken into account to correct the measured values to produce an atmospheric record.

[50] For CO_2 measurements, the correction for gravitational fractionation is small (lowering the measured CO_2 by up to 1.4 ppm at Law Dome and 2.5 ppm at South Pole, with a maximum uncertainty of 0.02 ppm) and has been calculated by multiplying the measured (or modeled when there was no measurement available) δ^{15}N of N_2 at any depth by the measured CO_2 concentration at the same depth, as follows [*Sowers et al.*, 1989]:

$$[CO_2]_{corr} = 10^{-3} \quad \delta^{15}\text{N} \quad (M_{CO_2} - M_{air}) \quad [CO_2]_{meas} \tag{5}$$

where $[CO_2]_{corrected}$ is the measured CO_2 concentration corrected for gravitational fractionation, M_{CO_2} and M_{air} are the molecular mass of CO_2 and air (44.01 and 28.96 amu, respectively).

[51] For δ^{13}C measurements, the correction for gravitational fractionation is more significant (lowering the δ^{13}C by

Table 2. Comparison of Performances of Graters 1 and 6[a]

Grater Number	Crushed Ice (%)	Air Released ($mL\ kg^{-1}_{crushed\ mass}$)	Air Released ($mL\ kg^{-1}_{initial\ mass}$)	ΔCO_2 (ppm)	$\Delta\ ^{13}C\text{-}CO_2$ ( )	$\Delta\ ^{18}O\text{-}CO_2$ ( )	ΔCH_4 (ppb)	ΔCO (ppb)	ΔN_2O (ppb)
1	84 (4)	85 (6)	71 (3)	–0.1 (0.9)	–0.05 (0.02)	0.5 (0.2)	5 (2)	6 (3)	0.6 (1.1)
6	73 (11)	99 (21)	71 (14)	1.3 (1.2)	–0.11 (0.10)	1.5 (1.4)	10 (7)	18 (10)	1.8 (0.7)

[a]The air released is expressed as either milliliter of air released over the mass of crushed ice (column 3, $mL\ kg^{-1}_{crushed\ mass}$) or milliliter of air released per kg of initial mass of ice (column 4, $mL\ kg^{-1}_{initial\ mass}$). The values in parentheses in columns 2–4 are the standard deviations over 33 crushed samples for grater 1 and 70 crushed samples for grater 6. ΔCO_2 (or $\Delta\ ^{13}CO_2$ or ΔCH_4, etc.) represents the difference between the mean measured and the expected CO_2 (or $^{13}CO_2$ or CH_4, etc.) value for BFI tests. The values in parentheses in columns 5–10 are the standard deviations over $n = 4$ BFI tests for grater 1 and $n = 15$ BFI tests for grater 6.

up to 0.3 at Law Dome and 0.6 at South Pole, with a maximum uncertainty of 0.03), and it is applied as a correction summed to the measured δ^{13}C. While the measured δ^{15}N of N_2 can be used to correct for gravitational fractionation, we have preferred to use the modeled δ^{13}C gravitational correction for the following reasons:

[52] 1. For high accumulation rate sites like DE08, the firn column does not reach equilibrium completely and there is a difference of $\sim$ 6% in the effect of gravity on N_2 and CO_2, due to different rates of diffusion relative to ice advection [*Trudinger et al.*, 1997], and the firn model is needed to quantify this.

[53] 2. We do not have many available δ^{15}N measurements in ice, to obtain consistent corrections for firn and ice.

[54] 3. At Law Dome, the measured δ^{15}N in firn generally exhibits more scatter than is expected. To our knowledge, there is no known firn process that can explain the measured variability; therefore, we considered it random analytical noise. Using the modeled output of the effect of gravity on δ^{13}C has been useful to avoid introducing additional scatter from δ^{15}N measurements to the δ^{13}C from the correction for gravitational fractionation.

[55] 4. At South Pole, the measured δ^{15}N shows a strong influence of the seasonal thermal gradient at 10 m depth [*Battle et al.*, 1996]. When we used the measured δ^{15}N to correct for the effect of gravity, the 10 m depth δ^{13}C would appear to be overcorrected, suggesting that a much smaller thermal effect exists for δ^{13}C (this is consistent with what is expected based on consideration of momentum transfer in collisions related to the symmetry of the CO_2 molecule; J. Severinghaus, personal communication, 2012). Thermal diffusion in the firn [*Severinghaus et al.*, 2001] is not represented in the CSIRO firn model.

[56] It is worth specifying that, for the work presented here, uncertainties associated with thermal diffusion in the upper part of the firn record do not affect the main results of our study (i.e., the overlap between ice and firn δ^{13}C measurements). Long-term thermal gradients are considered negligible, because seasonal temperature changes reverse semiannually [*Severinghaus et al.*, 2001], so that seasonal thermal gradients are vanishingly small with depth.

[57] Also, no size-dependent fractionation during bubble close off is taken into account in the present study, because CO_2 should not be affected [*Severinghaus and Battle*, 2006].

[58] To estimate the δ^{13}C gravitational correction to be applied as a function of depth, the firn model is run for $^{12}C\text{-}CO_2$ and $^{13}C\text{-}CO_2$ with constant CO_2 atmospheric levels. Our modeled δ^{15}N agrees with the measured one within 0.02 , except for South Pole 2001, where the difference was up to 0.05 for the deepest layers, providing evidence that our modeled gravity correction is accurate.

2.6.2. Diffusion Correction

[59] For measurements of isotopic ratios in firn and ice air samples, a so-called diffusion correction is needed [*Trudinger et al.*, 1997]. This correction arises from the fact that an isotope ratio is the ratio of two isotopes with slightly different diffusion coefficients and therefore slightly different effective ages [*Trudinger*, 2000, section 3.6]. For hypothetical species with constant isotopic ratio, but changing atmospheric concentrations, the isotopic ratio in the firn can be significantly different than the atmospheric ratio.

[60] The diffusion correction depends on the depth of the diffusive column in the firn; among the sites investigated in this study, it is lowest at DSSW20K and highest at South Pole.

[61] For δ^{13}C, the diffusion correction is proportional to the rate of change of CO_2 concentration, which makes the δ^{13}C diffusion correction insignificant in the LHPI; however, it is significant in the Industrial Period and is up to 0.26 in 1971 A.D. at South Pole (with a maximum 1σ uncertainty of 0.03).

[62] To calculate the diffusion correction, we need atmospheric histories of both CO_2 and δ^{13}C (or more correctly, $^{13}C\text{-}CO_2$); for this, we use smoothing spline fits to the ice core measurements of CO_2 and δ^{13}C. The diffusion correction is sensitive to the degree of smoothing chosen for the splines, and we factored this effect into our uncertainties. The diffusion correction is rather insensitive to the growth rate of the δ^{13}C smoothing spline [*Trudinger*, 2000].

[63] Finally, we estimated the uncertainty in the gravity and diffusion corrections with the ensemble of diffusivity parameters [*Trudinger et al.*, 2013], including among our parameter sets the possibility of dispersive mixing in the lock-in zone, which may arise from a nonuniform velocity distribution and viscous flow in the firn open porosity [*Buizert et al.*, 2012]. The uncertainties associated with the corrections for gravitational and diffusion fractionation from the CSIRO firn model (generally 1 or 2 orders of magnitude lower than the analytical uncertainty) were summed to the total analytical uncertainty to derive a combined standard uncertainty defined as the square root of the variance [*Joint Committee for Guides in Metrology*, 2008].

3. Results and Discussions

[64] In the following sections, we first present the results of our tests, as listed in section 2.2.2 (steps 1–5) and the tests performed to quantify the total analytical uncertainty. This leads us to the description of the criteria used to select new

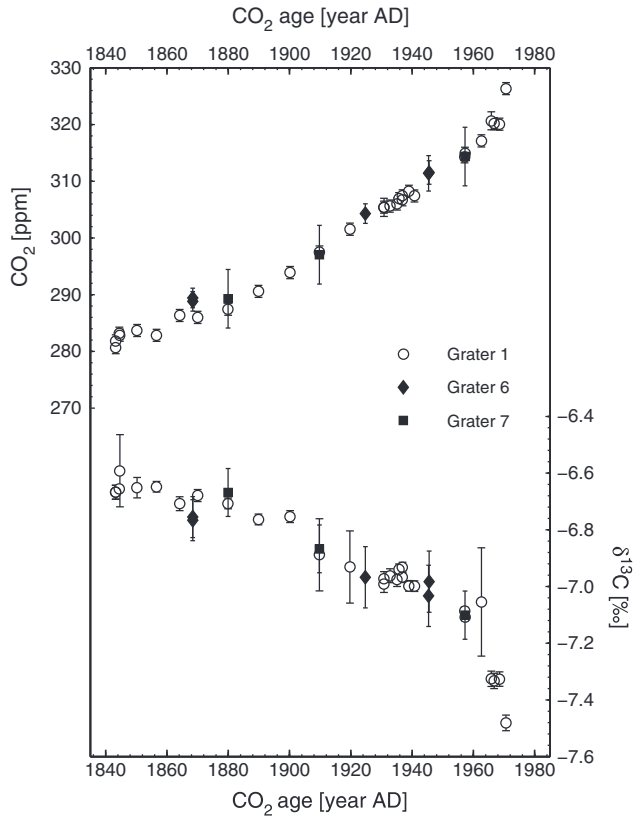

Figure 2. Comparison between different graters: CO_2 concentration (upper part) and δ^{13}C (lower part) measured in air extracted from ice with Graters 1 (open circles), 6 (filled diamonds), and 7 (filled squares) covering the period 1840–1970 A.D. Error bars are combined standard uncertainties described in the text (namely, $u_c(y)$).

and old measurements as well as the uncertainties attributed to each measurement. Then, we show our new δ^{13}C record in ice and compare it to firn and atmospheric measurements.

3.1. Precision and Uncertainty

3.1.1. Grater Testing and "Blank" Correction

[65] Of the three graters used in this study, grater 6 has been extensively tested with 106 tests performed. Grater 1 had already been tested for the *Etheridge et al.* [1996], the F99, and the *MacFarling Meure et al.* [2006] studies, and in this study, we have found results very similar to those previously reported. Table 2 summarizes the results obtained for the two graters when bubble-free ice (BFI, defined as ice containing no visible bubbles) tests were performed under the same conditions as when real ice samples were crushed (n = 15 for grater 6 and n = 4 for grater 1). Grater 7 showed results very similar to grater 6. We omit grater 7 from Table 2 because the small number of tests performed with it was not sufficiently constraining.

[66] The two ice graters compared in Table 2 showed different crushing efficiency. Most of an ice sample is crushed into chips, but a small amount (100–300 g) of ice remains intact. Grater 1 shows higher crushing efficiency (expressed as a percentage of crushed ice in Table 2) probably because, thanks to the larger volume available, the chips do not fill the entire volume. On the other hand, because it has bigger holes than grater 6, grater 1 produces larger chips so that grater 6 shows higher amount (mL) of air extracted per kg of crushed ice (Table 2). As a result of these two competing effects, the amount of air extracted from samples of the same size (mL of air per kg of initial mass of ice in Table 2) is on average the same for the two graters.

[67] We define a "blank" correction as the difference between the expected and the measured CO_2 concentration and δ^{13}C when running BFI tests (Table 2). The BFI tests showed that blank corrections should be applied independently for each grater. Grater 1 showed the smallest and generally least variable blank for all measured species.

[68] When corrected for their respective blanks, the three graters gave consistent (within uncertainty) CO_2 and δ^{13}C results for ice cores (Figure 2).

[69] The error bars attributed to each measured sample shown in Figure 2 are estimated based on the standard deviations listed in Table 2. Thus, according to Table 2, the samples extracted with grater 1 (open circles in Figure 2) generally have the smallest δ^{13}C uncertainty (0.02). Just four of those measurements show large uncertainty (0.13). They were performed in a period when high variability was found when running BFI tests, traced to the aged indium seals used in grater 1. To improve reproducibility, the indium seals were completely replaced after each set of four extractions (corresponding to 1 day, as mentioned at step 4 in section 2.2.2).

3.1.2. Trap Storage

[70] When running BFI tests, we found that the difference between the expected and measured $\delta^{46}CO_2$ ratio depended on the time elapsed between extraction and analysis (see section A5). This affected the measured δ^{13}C as well (see Figure A1). To minimize the effect, we reduced the storage time by measuring each sample straight after extraction (typically, less than 1 h for the GCs and less than 12 h for the IRMS analysis). This resulted in keeping the alteration of the δ^{18}O as low as 0.5 and reproducible within 0.2 , which should have a negligible influence (less than 0.02) on the measured δ^{13}C.

[71] We also dried and evacuated the –100 C water trap after each extraction (as mentioned at step 3 in section 2.2.2) to try to maximize the amount of water removed from the air sample.

3.1.3. Quantifying Uncertainty

[72] The total analytical uncertainty associated with storage and preparation of ice samples, extraction, and analysis of gas was determined in three different ways:

[73] 1. Comparing two to three air samples extracted from ice collected at the same depth (only possible for the large diameter DE08 core). This allowed us to estimate the variability due to the combination of horizontal heterogeneity of an ice core, and extraction and analysis of air from one ice core. We found an average reproducibility (measured as the pooled standard deviation over two or three replicates) of 0.03 for δ^{13}C and of 0.2 for δ^{18}O over n = 3 (three depths × two replicates for each depth) extracted with grater 1 and of 0.06 for δ^{13}C and of 0.7 for δ^{18}O over n = 5 (three depths × two replicates + two depths × three replicates) extracted with grater 6.

[74] 2. Collecting and analyzing air of known composition injected in the grater before (and kept in it while) crushing BFI. Three differently produced BFI were tested

(details of the BFI used and the results obtained are given in section A6 and Figure A2). This was our best way of estimating the precision and accuracy of our extraction procedure by simulating the extraction of our reference air from ice (see values in parentheses in Table 2). The similarity of the precision obtained when simulating the extraction process with BFI to the replicates-based precision (described at step 1) gives us confidence that the assumption of horizontal homogeneity in the ice core at any given depth is valid and that our estimated reproducibility primarily reflects the characteristics of our extraction and analysis procedure (with no major influence from the ice sampling and storage). On the basis of these results, the analytical uncertainty attributed to each sample was estimated from the reproducibility measured for BFI tests (as in Table 2), over periods of time when no significant change in the extraction procedure occurred.

[75] 3. Finally, the variability associated with different cores sampled at the same or at different sites was estimated by measuring the scatter of the results obtained from ice of similar age, confirmed by the χ^2 (chi-squared) statistics of the Kalman filter double deconvolution [*Trudinger et al.*, 2002b]. We found that variability (1.2 ppm for CO_2 concentration and 0.05 for $\delta^{13}C$) to be higher than the sum of the analytical uncertainty plus the uncertainty associated with gravity and diffusion correction for most samples. The variability associated with different cores was selected as the minimum uncertainty to be used in the Kalman filter double deconvolution when estimating sinks and sources of atmospheric CO_2 (see section 3.4).

3.2. Results Selection

[76] The selection of the data plays an important role in the production of a reliable and accurate data set. It has been especially important in the current study, because measurements carried out over a period of 20 years have been compared and combined into one data set. Old and new measurements were selected according to the same selection criteria.

[77] Selection of firn measurements was based on:

[78] 1. A pairwise agreement criteria between flasks of air sampled at the same depth: measurements of pairs of flasks sampled at the same depth were rejected if different by more than 0.1 in $\delta^{13}C$.

[79] 2. Development of a consistent set of rules to judge the reliability of the analysis: measurements with $\sigma >$ 0.04 for $\delta^{13}C$ and $\sigma > 0.08$ for $\delta^{18}O$ were rejected (where σ is the standard deviation over eight acquisitions performed on one sample at the IRMS). This threshold for rejection was chosen based on the typical reproducibility of our IRMS over eight acquisitions: 0.02 for $\delta^{13}C$ and 0.04 for $\delta^{18}O$, with 2× larger tolerance to account for the variability introduced by the sampling procedure.

[80] Selection of ice core measurements consisted of three independent parts:

[81] 1. Selection of ice samples of good quality for air storage and extraction: ice samples were carefully scrutinized prior to extraction and only samples free from melt layers were selected; also, ice samples near close off were selected only from ice layers formed from winter snow because summer layers are known to have significantly higher open porosity and summer ice samples from shallow depths may not be fully closed off.

[82] 2. Satisfying the minimum requirements of the extraction of air from ice procedure in terms of pressure measured in the extraction line, temperatures of the ice sample, water trap and sample trap, and time elapsed between extraction and analysis. Samples that had remained in the sample trap for more than 24 h between extraction and analysis were rejected, based on the results shown in Figure A1. Most of the samples used in the F99 study were analyzed immediately after extraction (<12 h).

[83] 3. Development of a consistent set of rules to judge the reliability of the analysis: measurements with $\sigma >$ 0.06 for $\delta^{13}C$ and $\sigma > 0.12$ for $\delta^{18}O$ were all rejected (where σ is the standard deviation over eight acquisitions performed on one sample at the IRMS). The threshold for rejection was chosen based on the results of $\Delta\delta^{13}C$-CO_2 shown in Table 2, with 3× larger tolerance, to account for variability introduced by the sampling and extraction procedures; most measurements rejected according to this criterion corresponded to samples of the F99 data set that were found to be contaminated (in the F99 paper, the contaminant was tentatively identified with a contribution in the IRMS to mass 45, 46, and 44 coming from the ethanol used to cool down the water trap of the extraction line, which was inadvertently stored in the ICELAB cold room).

[84] As for the F99 record, a $\delta^{13}C$ measurement was rejected if the amount of extracted air was insufficient to provide a signal of at least 6 nA (corresponding to 2 V at 3×10^8) in the cup measuring mass 44 of the MAT252, and analyses with a sample to standard voltage ratio outside of the selection range of 0.9 ± 0.1 were rejected (see section A7 for details).

[85] Finally, the measured CH_4, N_2O, and CO concentrations were used as checks of the reliability of the sampling/extraction/analysis procedure. This was done by comparing the measured CH_4, N_2O, and CO concentration to the value of the spline fit to all selected data, corresponding to the age of each sample. Values clearly different from the spline were flagged, and the measured $\delta^{13}C$ rejected when the cause for the difference could be identified. In particular, high CO concentrations were caused by contamination with organic material (i.e., drilling fluid, which can possibly also affect the $\delta^{13}C$, due to the production of isobaric molecules to CO_2, in the ion source of the IRMS). Low values of both CO_2 and N_2O were generally associated with warming to near melting point of the ice after drilling (CO_2 and N_2O being the most soluble among the measured gases). Ice samples near close off with significant open porosity often showed unrealistically high values for more than one species, including CH_4.

[86] Out of a total of 194 samples measured for $\delta^{13}C$ since ice core measurements began at CSIRO in 1993, only 69 $\delta^{13}C$ measurements have been retained using these selection criteria, reflecting the difficulty of making these analyses precisely and accurately. Of the 125 $\delta^{13}C$ rejected measurements, 63 among 99 measurements were from the F99 study, whereas 62 among 95 measurements were from the current study. The highest number of rejections (28) are due to the organic contamination described in F99, attributed to the ethanol used to cool down the water trap. Almost as many measurements (27) have been rejected due to long storage time in the sample trap between extraction of air from ice and analysis, affecting the $\delta^{46}CO_2$ (most of those

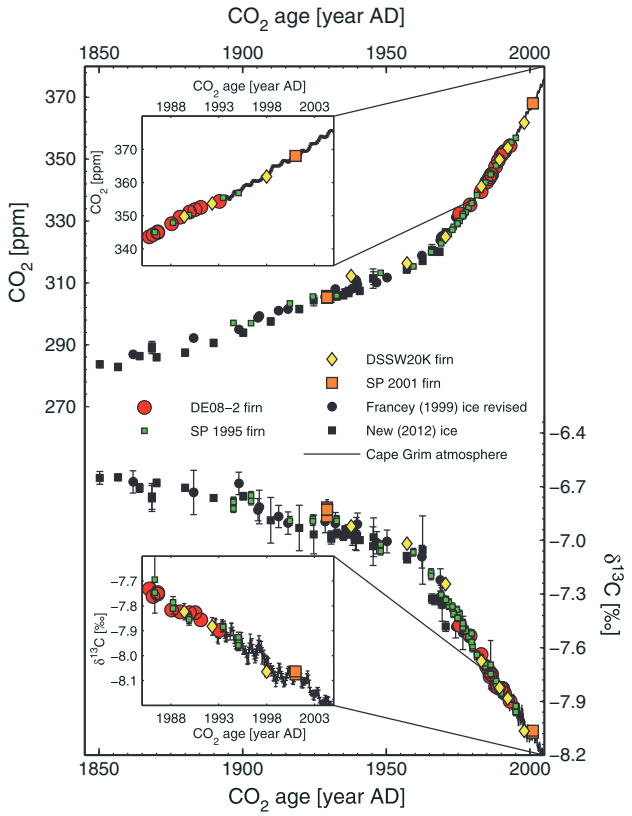

Figure 3. Comparison between ice, firn, and direct atmospheric measurements: firn measurements are in color (red circles: DE08-2 - 14 points; green squares: South Pole 1995 - 58 points; yellow diamonds: DSSW20K - 6 points; open red squares: South Pole 2001 - 8 points); ice measurements are in black (filled circles: selected and revised ice measurements from F99 - 21 points; filled squares: new ice measurements - 30 points); the line connects monthly mean values of atmospheric measurements at Cape Grim. Error bars are as follows: ice measurements, total uncertainties (analytical + gravity and diffusion correction) as described in the text; firn measurements, uncertainties from gravity and diffusion correction summed to standard deviations over n replicated analyses when $n > 6$ or difference between minimum and maximum measured values for $n < 6$; and atmospheric measurements, the standard deviations for the monthly means are calculated from the standard deviation of the monthly mean from the daily smooth curve values and the standard deviation of the residuals of each data point about the smooth curve for that month (typical uncertainty is 0.015).

measurements were from the current study). The third most significant cause of rejections (22) was due to the small signal produced during the IRMS analysis, related to the small amount of air extracted or residual after GC analysis. Many samples (18) showed unrealistically high CO concentration, suggesting a leak or contaminated core. A lower number of measurements have been rejected because of evidence of leaking during extraction (9), post coring melting (4), or an unbalanced sample to standard ratio during IRMS analysis that caused an unacceptable bias (3). Finally, 14 measurements have been rejected based on unrealistically high CO_2 when compared to the results from samples of same or similar age, which would imply implausible atmospheric signals, especially given the smoothing of the air age by diffusion and bubble formation.

[87] The same selection criteria applied to the BFI tests allowed an accurate quantification of the blank correction to be applied to old and new δ^{13}C measurements. Of the 129 BFI tests measured for δ^{13}C, 9 were rejected because of problems during the extraction procedure (four leaked, three technical issues, and three contaminated BFI) and 31 were rejected because of issues regarding the IRMS analysis (22 high storage time, 2 low voltage, and 7 poor reproducibility of replicated acquisition on the IRMS). Generally, issues with BFI tests caused a difference from the target value to be more than 0.1 . The blank correction was found to be much smaller (0.03) than the one applied in the F99 study (0.11). This is the main contributor to the difference (on average 0.17) between the previous and the revised Law Dome data sets.

3.3. The New ^{13}C Record

[88] When the F99 data set was published, it represented the only high precision published data set of δ^{13}C from ice cores over the last 1000 years that could be compared to firn and direct atmospheric measurements. The overlap between ice and firn was used to show that the ice record was compatible with direct atmospheric measurements. The overlap between firn and direct atmospheric measurements from Cape Grim covered a significant number of years (1980–1993 A.D.). The overlap between ice and firn measurements from Law Dome in F99 was based on a much smaller number of points. *Trudinger* [2000, p. 108] showed that there was a significant discrepancy between the F99 data set and the firn δ^{13}C record from the firn campaign performed at the South Pole in 1995, with the F99 measured values being 0.1–0.2 higher than the values measured in South Pole firn air. Even though a number of possible causes were offered, no convincing explanation was found.

[89] Figure 3 shows the comparison of our new ice core data set with firn measurements from DE08-2, DSSW20K and South Pole, and the Cape Grim atmospheric record.

[90] When δ^{13}C is plotted versus effective age of samples from different sites, the new ice measurements are compatible (within uncertainties) with the firn record from South Pole. Each site has a different age distribution—South Pole firn air has a spread in age that is 4 times that of DE08 and DE08-2 and 2–3 times that of DSS and DSSW20K, for CO_2 dated 1940 A.D. (see Table 1), and this will lead to some differences in δ^{13}C of the same age from different sites.

[91] Only a few δ^{13}C measurements of shallow ice (corresponding to the period 1965–1975 A.D.) are not consistent with the firn record within their uncertainties. Ice near close off could have significant open porosity which, when brought to the surface, could trap significant amounts of air from modern atmosphere, thus lowering the measured δ^{13}C [*Aydin et al.*, 2010]. Figure 3 shows the overlap of firn and direct atmospheric samples from Cape Grim (inset).

[92] As an independent test of the robustness of the inferred atmospheric histories of δ^{13}C, we employed a separate set of δ^{13}C firn air measurements, along with the Bowdoin firn air model (see section 2.4 above). In this test, we used our inferred histories to drive both the Bowdoin

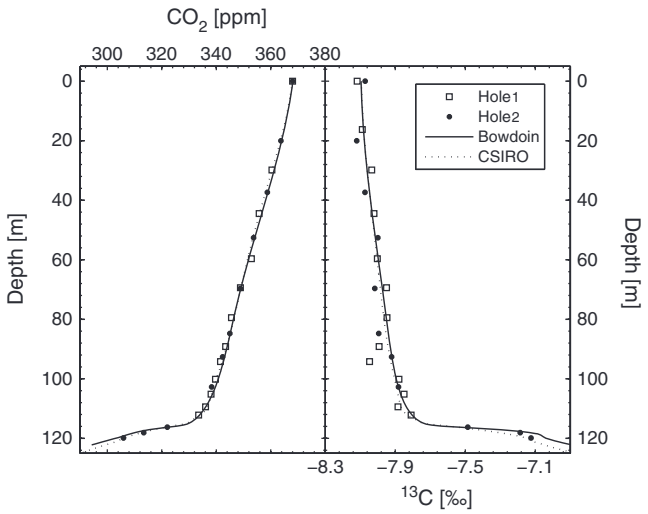

Figure 4. CO_2 and δ^{13}C profiles (versus depth) for South Pole 2001 firn: firn air was sampled from two holes (white squares and filled circles, error bars are smaller than the size of the symbols). CO_2 concentration was measured at NOAA/CMDL, δ^{13}C measurements were performed at INSTAAR. The data have been corrected for gravitational fractionation using the measured δ^{15}N of N_2. No correction for diffusion fractionation was needed because the model takes that into account. The modeled CO_2 and δ^{13}C profiles are shown as lines (solid line: Bowdoin college, dotted line: CSIRO).

and the CSIRO firn model forward in time and compared the model predictions of the depth profile of firn air composition with a set of flasks collected from firn at the South Pole in 2001. The flasks analyzed at INSTAAR were corrected for 0.08 scale offset measured between CSIRO and INSTAAR. The models were independently calibrated to match measurements of CO_2, CH_4, and δ^{15}N of N_2 at South Pole 2001. South Pole firn measurements were not used to construct the atmospheric histories driving the firn model. Results of this test are shown in Figure 4.

[93] The agreement of model and data provide strong evidence of the robustness of the atmospheric reconstructions and is further evidence of the consistency of:

[94] 1. δ^{13}C measurements from ice and firn sampled at different sites.

[95] 2. δ^{13}C measurements from different laboratories, when scales offsets are allowed for.

[96] 3. Different models used to simulate the diffusion of air in firn.

[97] Finally, Figure 5 shows the revised record of CO_2 concentration and the new record of δ^{13}C over the last 1000 years, with Figure 6 presenting the details of the record after 1840 A.D.

[98] The main features of the previously published CO_2 and δ^{13}C records [*Etheridge et al.*, 1996; *Francey et al.*, 1999; *MacFarling Meure et al.*, 2006] remain essentially unchanged. However, the higher sample density in the twentieth century provides more certainty on the data (Figure 6). A recent study using ice from the West Antarctic Ice Sheet (WAIS) has confirmed the main features of the Law Dome CO_2 record but has shown a smoother decrease of the CO_2 concentration around 1600 A.D., possibly caused by a higher degree of signal smoothing in WAIS ice during bubble close off compared to Law Dome [*Ahn et al.*, 2012]. Furthermore, the mean CO_2 LPIH level has been found to be, on average, 3 ppm higher at WAIS, which could point toward significant (even though small) in situ production of CO_2 [*Tschumi and Stauffer*, 2000] in the ice at WAIS.

[99] Data from Dome Fuji firn air and direct atmospheric measurements from Syowa station [*Sugawara et al.*, 2003] show a flattening of δ^{13}C between 1990 and 1997/1998 which is not in agreement with the annual (seasonality suppressed) Cape Grim record which decreases from 1992 to 1999. However, the Cape Grim record is extremely closely

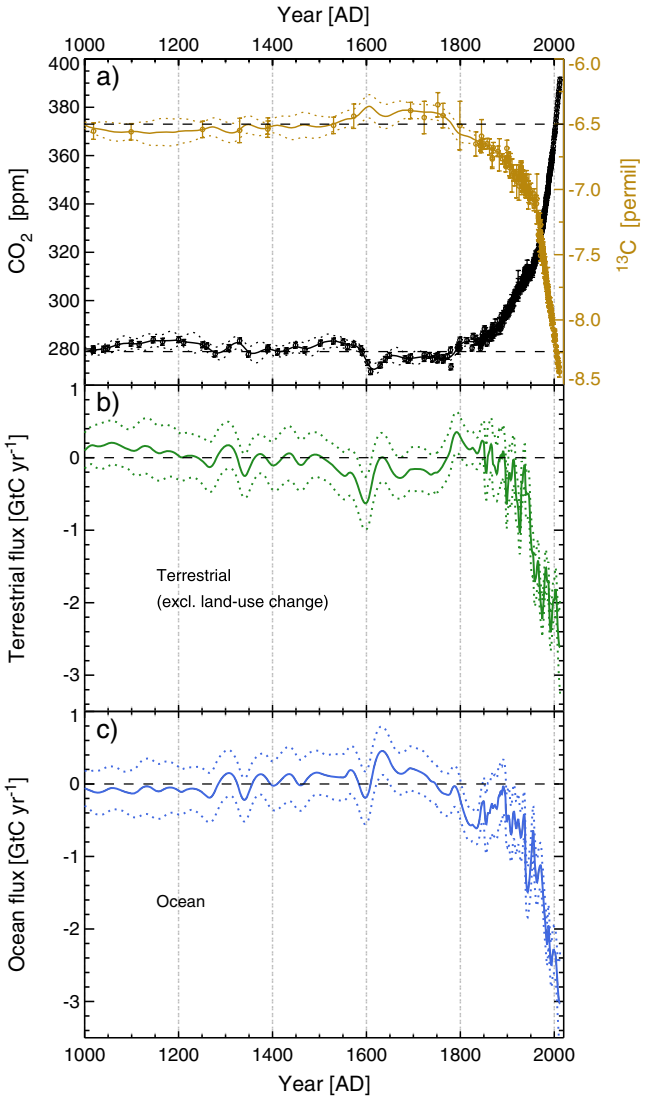

Figure 5. The new records between 1000 and 2012 A.D.: (a) CO_2 concentration (black circles) and the δ^{13}C (brown circles); solid lines are results of the double deconvolution for, respectively, (b) the atmosphere-terrestrial biosphere and (c) the atmosphere-ocean CO_2 flux. Error bars are analytical uncertainties when the analytical uncertainty was larger than the minimum uncertainty (1.2 ppm and 0.05) as described in the text (section 3.1). Dashed lines show the 1σ uncertainty associated to the KFDD.

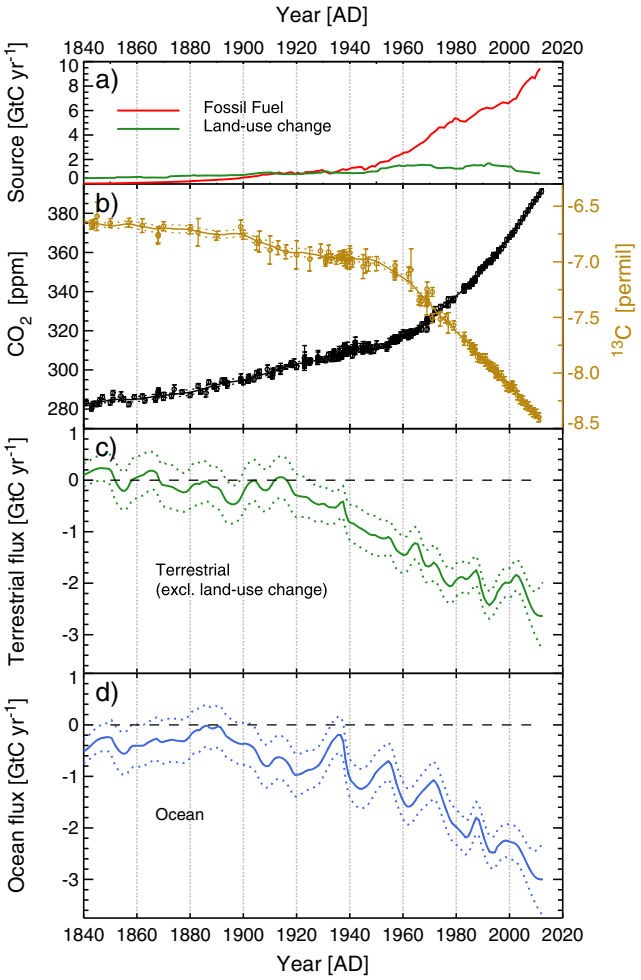

Figure 6. The new records between 1850 and 2012 A.D.: (a) prescribed fossil fuel (red) and land use change (green) histories; (b) CO_2 concentration (black circles) and the δ^{13}C (brown circles); solid lines are results of the double deconvolution for, respectively, (c) the atmosphere-terrestrial biosphere and (d) the atmosphere-ocean CO_2 flux. Error bars are analytical uncertainties when the analytical uncertainty was larger than the minimum uncertainty (1.2 ppm and 0.05) as described in the text (section 3.1). Dashed lines show the 1σ uncertainty associated to the KFDD.

matched (seasonally and annually) over the period with four Antarctic and sub-Antarctic sites (South Pole, Casey, Macquarie Island, and Mawson) [*Francey et al.*, 2013]. Additionally, from 1992 through to 2012, same air flask comparisons involving flasks filled at Cape Grim and analyzed by both CSIRO and NOAA laboratories [*Masarie et al.*, 2001] give closely similar results; all show the same decreasing annual mean δ^{13}C from 1992 to 1999. Given the weight of this independent evidence, we accept the Cape Grim record as more representative of Antarctic air.

3.4. Implications for the Interpretation of the Global C Cycle

[100] We used a KFDD [*Trudinger et al.*, 2002b] of the new data sets shown in Figure 5 to attribute the CO_2 and δ^{13}C variations to land and ocean fluxes. All the main features found from the KFDD of the previous records are confirmed and are described in the following sections.

3.4.1. Preindustrial

[101] Between 1000 and 1600 A.D., the CO_2 concentration varies between 278 and 284 ppm. At the same time, between 1000 and 1500 A.D., the δ^{13}C stayed relatively constant around –6.55 . Around 1600 A.D., the Law Dome CO_2 ice core record shows a prominent decrease in concentration. Currently, there are no reliable δ^{13}C measurements in the Law Dome ice core record for this time. We can therefore estimate the total fluxes of carbon well, but not the partition between ocean and land. Although the KFDD gives an estimate for δ^{13}C around 1600 A.D., this is based simply on correlations in the covariance matrix and should not be interpreted as a real signal. CO_2 subsequently increases a little to 1650 A.D. but stays low until about 1750 A.D. This period of low CO_2 coincides with high δ^{13}C interpreted by the KFDD as terrestrial uptake, which could be caused by a decrease of the Northern Hemispheric or global surface temperature [*Mann et al.*, 2008; *Oppo et al.*, 2009] during the Little Ice Age. *Trudinger et al.* [1999] suggested that the lower temperature reduced both the release of CO_2 (soil respiration) and the uptake (photosynthesis) of CO_2 by the terrestrial biosphere, with the respiration reduction dominating, causing the terrestrial biosphere to accumulate carbon. Lower atmospheric CH_4 was found to be a likely result of land surface cooling during that period [*Etheridge et al.*, 1998; *Ferretti et al.*, 2006; *Mitchell et al.*, 2011].

[102] The preindustrial level of δ^{13}C in our record is –6.50 , on average 0.17 lower than in F99. This change is around 10% of the δ^{13}C decrease from the preindustrial to the present (Figure 5). Models of the carbon cycle that have been used to estimate C fluxes from the δ^{13}C and CO_2 variation over decades to centuries [e.g., *Joos et al.*, 1999; *Trudinger et al.*, 2002b] have uncertainty in a number of their model parameters that can change the modeled LPIH-to-contemporary δ^{13}C by a similar amount without changing recent net uptake by the land and oceans. These parameters include the residence times of both the terrestrial and ocean reservoirs, including the gas exchange coefficient for exchange between the atmosphere and ocean, variation in global isotopic fractionation due to temperature or the conversion of C_3 to C_4 ecosystems due to change in tropical land use [*Joos and Bruno*, 1998; *Ciais et al.*, 1999; *Trudinger et al.*, 1999]. Therefore, the reduced mean LPIH δ^{13}C level is unlikely to lead to any significant change in estimated C fluxes but is expected to require different combinations of these model parameters that match the observed CO_2 and δ^{13}C. It may, however, have implications for studies like *Krakauer et al.* [2006] or similar, which use the preindustrial atmospheric δ^{13}C to learn about this parameters.

[103] We emphasize that δ^{13}C measurements are much sparser than CO_2 measurements during the LPIH (see Figure 5). A higher sample density survey is underway for the LPIH to be able to infer the sources and sinks of CO_2 during this important time with higher confidence and time resolution. Our major future objective is to increase the time resolution of δ^{13}C data points around 1600 A.D. to explain the cause of this prolonged event of rapid C uptake.

3.4.2. Industrial

[104] During the Industrial Period, two distinct slopes of CO_2 growth (and corresponding δ^{13}C decrease) can be dis-

tinguished (Figure 6) before and after 1960 A.D. due to an acceleration of the release of anthropogenically derived CO_2 with the postwar economic boom [*Rafelski et al.*, 2009].

[105] The ocean and the terrestrial biosphere carbon fluxes were significantly larger in the Industrial Period than during the LPIH. Ocean and land both became strong sinks of CO_2 because of the effect of the increasing atmospheric CO_2 on those carbon pools.

[106] A flattening of the atmospheric CO_2 concentration around 1940 A.D. (1935–1950 A.D.) was highlighted in the *Etheridge et al.* [1996] and *MacFarling Meure et al.* [2006] papers. The F99 record showed a flattening in $\delta^{13}C$ starting well before the one seen in the CO_2 concentration record. Our new record confirms the significant flattening of $\delta^{13}C$ during the period 1915–1950 A.D. (Figure 6). *Trudinger* [2000, section 6.4] and *Trudinger et al.* [2002b] looked in detail at the 1940s flattening in CO_2 and the simultaneous $\delta^{13}C$ variation. Taking into account the effect of firn diffusion and bubble trapping, they concluded that these CO_2 and $\delta^{13}C$ variations required almost 3 GtC/yr uptake around 1945–1948 that was mostly oceanic, but could have been up to one third biospheric. Note that the firn processes not only smooth atmospheric variations but also cause a shift in the effective age when the atmospheric growth rate departs rapidly from linear [*Trudinger et al.*, 2002a]; for the 1940s flattening, we believe that the atmospheric event probably occurred around 5 years later than is indicated in the ice core record dated with constant gas-age/ice-age difference.

[107] The double deconvolution applied to the new record also suggests a major role for ocean uptake at this time. This is in contrast with the analysis of *Rafelski et al.* [2009], whose single deconvolution attributed this feature mostly to land processes. However, the lack of increase in $\delta^{13}C$ during the 1940s implies that land uptake or underestimated fuel emissions were not the dominant cause of the CO_2 flattening. *Trudinger et al.* [2002b] concluded that more $\delta^{13}C$ measurements with improved precision were needed to confirm the ocean as a significant sink in the 1940s. Around 1940, our new $\delta^{13}C$ record has similar scatter and uncertainty to the F99 record, so provides a similar constraint. Reduction in uncertainty in $\delta^{13}C$ at this time is still needed to confirm our conclusion. The role of the ocean in the 1940s is rather interesting since the terrestrial biosphere is usually thought to be responsible for short-term (decadal) atmospheric CO_2 variations, and will require further investigation in the future to understand the cause of the increased ocean uptake (biochemical causes such as the dust peak measured in Antarctic ice (J. McConnell, personal communication, 2012) or physical causes such as ocean circulation).

[108] Further analysis of these CO_2 and $\delta^{13}C$ variations would ideally use age distributions to represent the firn processes, which would allow consideration of smoothing as well as time shifts of growth rate variations. The KFDD does not take into account climatic and land use change effects on isotopic discrimination by the terrestrial biosphere [*Randerson et al.*, 2002; *Scholze et al.*, 2003, 2008]. We tuned the carbon cycle model to match the latest GCP (Global Carbon Project) net fluxes for recent decades, so this omission is not expected to be a significant problem for the long-term (i.e., preindustrial to modern) change in net fluxes. However, it could contribute to errors in our estimated fluxes on decadal timescales, particularly if changes in discrimination due to climate cause significant variability in $\delta^{13}C$ but not CO_2. Also, any biases in the assumed fossil fuel emissions over the last 20–40 years [*Francey et al.*, 2013] could alter the inferred partitioning.

4. Conclusions

[109] The new $\delta^{13}C$ record covering the last 1000 years presented in this study revises earlier measurements and provides new ice core and firn air measurements from multiple sites. We have shown four independent lines of evidence showing that our new record is a true representation of the past atmosphere:

[110] 1. Consistent results when using three different extraction graters to extract air from ice;

[111] 2. New blank correction quantified through bubble-free ice (BFI) tests selected according to the sample results selection;

[112] 3. New measurements since 1845 A.D. consistent with the previously published measurements reassessed through the new selection and correction procedures;

[113] 4. An improved and extended overlap of the results from ice cores, firn, and atmospheric samples, including new firn model corrections and firn samples measured at another laboratory and compared with output from a different firn model.

[114] The overlap resolves previously observed discrepancies between Law Dome ice and South Pole firn, giving better confidence in the ice archive for $\delta^{13}C$. Our revised preindustrial $\delta^{13}C$ level is –6.5 . The main CO_2 fluxes estimated through a Kalman filter double deconvolution remain essentially the same as in previous publications. Our data set has relevance for models of carbon-climate feedbacks (e.g., Paleo Carbon Modeling Intercomparison Project, http://www.bridge.bris.ac.uk/projects/pcmip/introduction.html) and provides an atmospheric reference record for works aimed at studying the problem of in situ production of CO_2 in Greenland ice by means of the C stable isotopes [*Francey et al.*, 1997; *Tschumi and Stauffer*, 2000].

[115] We are now in the position to extend our $\delta^{13}C$ record back in time (before 1000 A.D.) with higher confidence and increase the sample density during the last 1000 years where significant changes of the CO_2 concentration occurred (e.g., Little Ice Age).

Appendix A: Experimental

A1. Grater Characteristics

[116] All extraction vessels were cylindrical, with a smaller diameter cylindrical grater welded on the inside. They feature a space, between the internal grater and the external container where chips produced by the grating action fall to avoid clogging the grater. Grater 1, also used in earlier studies [*Etheridge et al.*, 1996; *Francey et al.*, 1999; *MacFarling Meure et al.*, 2006], consists of a single cylindrical container sealed with two end caps by means of indium wire. The ice grater is welded to one end cap. Graters 6 and 7 feature two symmetrical cylindrical halves joined in the middle, sealed with copper gaskets (Conflat®) . For grater 6, the ice grater is welded to one part and is as long as the container. Grater 7 contains an ice grater, half the total length of the container, welded in each half of the container. The volume of grater 1 is 5.1 L and can contain an ice sample up to

17 cm long and 12 cm diameter. The volume of grater 6 is 3.2 L and can contain an ice sample up to 18 cm long and 9 cm diameter. The volume of grater 7 is 5.3 L and can contain an ice sample of up to 30 cm long and 9 cm diameter. Other graters (numbered 2 to 5) were tested in the past, but they were not used in the current study.

A2. GC Measurements

[117] A Series 400 CARLE/EG&G (Tulsa, Oklahoma, USA) gas chromatograph with flame ionization detector was used for the measurement of CH_4 and CO_2 (converted to CH_4 using a nickel catalyst at 400 C). A Trace Analytical RGA3 (Menlo Park, California, USA) gas chromatograph was used to measure CO with mercuric oxide reduction gas detector, which reduces HgO to Hg for detection by UV absorption. N_2O measurements were performed on a Shimadzu GC-8AIE (Kyoto, Japan) with electron capture detector. The raw measurement precision (1σ) based on the long-term, mean standard deviation of repeat aliquots from high-pressure cylinder working standards is 0.09 ppm for CO_2, 2.3 ppb for CH_4, 0.6 ppb for CO, and 0.3 ppb for N_2O [*Francey et al.*, 1996]. Revisions of the calibration scale between the measurements performed for the F99 study in 1993–1995 and our new measurements have produced differences of less than 0.6 ppm for CO_2.

[118] In general operation, air samples in flasks, tanks, and cylinders (typically in excess of 800 mL) are automatically injected and analyzed on the GCs using carousel autosamplers to ensure reproducibility and minimum sample consumption. Because of the limited amount of air available, a semiautomatic procedure was required to inject the small volume of ice core air samples into the GCs carousels [*Etheridge et al.*, 1988]. Roughly 15–20 mL were used to measure the concentration of CO_2, CH_4, and CO, and 12–15 mL were used to measure the concentration of N_2O. The remaining air (typically 40 mL) was used for $\delta^{13}C$ and $\delta^{18}O$ measurements.

A3. Calibration Scale Changes for ^{13}C

[119] When comparing measurements performed almost 20 years apart, rigorous traceability in the propagation of calibration scales becomes an important factor. The calibration scale used in the F99 study required manual correction for many artifacts for $\delta^{13}C$ and $\delta^{18}O$ measurements that have been extensively studied and quantified resulting in the CSIRO2005 calibration scale [*Allison and Francey*, 2007]. A recent revision (to be published elsewhere) of some of the identified shortcomings of the previous methods [*Francey et al.*, 1999; *Allison and Francey*, 2007], now incorporating a revised ion correction procedure [*Brand et al.*, 2010] in addition to better temporal understanding of many artifacts, has improved the calibration and propagation of all measurements.

[120] To propagate the calibration over time and apply calibration scale changes to samples, CO_2 in air standards (Southern Hemisphere baseline marine air) are routinely measured in a sequence together with samples. By expressing the isotopic ratio of CO_2 extracted from air samples relative to bracketing values of CO_2 extracted from an air standard using the same extraction equipment and extraction parameters, a number of potential systematic biases are minimized. A Primary Laboratory Air Standard (PLAS) used to define the current CSIRO $\delta^{13}C$ scale was calibrated against the NBS-19 in July 2009. The calibration of PLAS is then transferred to every other air standard by comparing analyses made directly against the PLAS where possible, or by analysis against the shortest path calibration, e.g., against a tank calibrated against a tank directly analyzed against the PLAS. This calibration extends into the past to include all air standards. For those with a drifting values, a revised drift rate was determined and the consistency over time established.

[121] The newly revised scale propagates errors from analysis and calibration such that the uncertainty estimate provided for each sample is a true estimate (at 90% confidence level) of the uncertainty in the difference between two samples. At each step, the uncertainty of each value assignment is revised through a consideration of the analytical precision of the measurement, the statistics of the intercalibration, i.e., how many analyses of each tank, the uncertainty of the standard value assignment (that includes a consideration of these steps in its own value assignment). This uncertainty is then incorporated into the measurement uncertainty for each sample. The absolute level of the Vienna Peedee belemnite (VPDB) calibration is still based on the analysis of NBS-19 CO_2 gas. To minimize the errors and to facilitate recalibration and uncertainty analysis, the calibration is automated within a SQL (Structured Query Language) database.

[122] Instrument performance for (early) samples analyzed without air standards is estimated and applied. This has allowed samples that were manually corrected in F99 to be treated in the same way as modern samples. All corrections are now consistently applied and can be easily reapplied if necessary to all ice core samples, all firn air samples, all modern air samples, and all calibration tanks.

A4. Cross Contamination

[123] Mixing of sample and reference gases in the ion source of an IRMS occurs when the IRMS is run in dual inlet mode. The size of this effect depends on the difference of $\delta^{45}CO_2$ and $\delta^{46}CO_2$ between sample and reference, on the idle time (the time allowed for a flow of gas to purge and equilibrate in the ion source before signal acquisition), and on the amount of sample.

[124] The range of $\delta^{46}CO_2$ of air in ice cores and firn is due to modification with depth from O-exchange with H_2O [*Assonov et al.*, 2005], which makes the $\delta^{46}CO_2$ of air in ice significantly more negative than that of atmospheric air (depending on the age/depth of a sample). For our measurements of modern atmospheric air, firn air, and ice core air against the pure CO_2 reference gas, $\delta^{45}CO_2$ varies between –2 (modern air) and 0 (ice) while $\delta^{46}CO_2$ varies from +14 (modern air) to –14 (ice). Therefore, when measuring CO_2 extracted from ice cores, the cross contamination is likely to affect the $\delta^{46}CO_2$ more than $\delta^{45}CO_2$ resulting in the introduction of scatter and possible bias in $\delta^{13}C$. While no correction for this effect was performed in the F99 study, the cross contamination is now much better understood and continually monitored, and a correction is applied to all data.

A5. Effect of Time Between Extraction and Measurement on $^{46}CO_2$

[125] When running BFI tests, we found that the difference between the expected and the measured $\delta^{13}C$ and $\delta^{18}O$

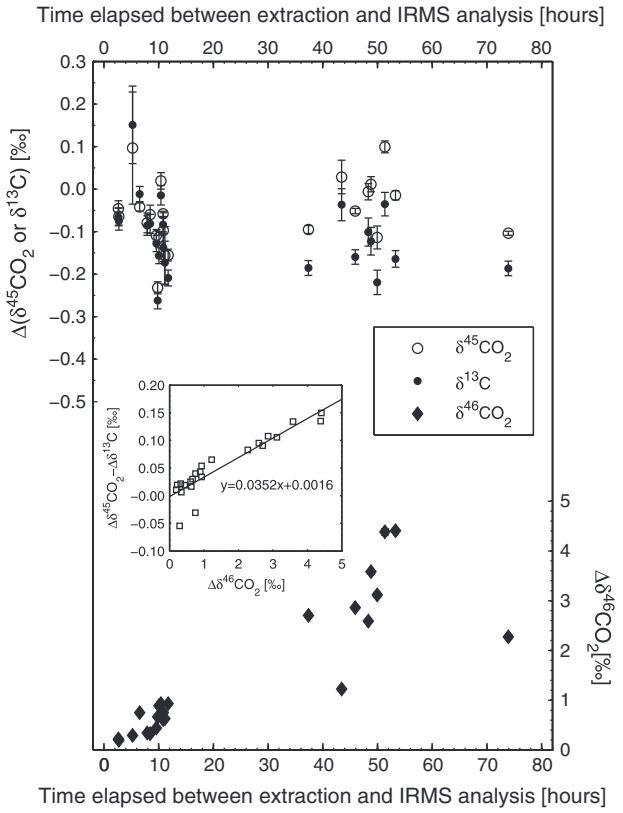

Figure A1. Oxygen isotope effect in the sample trap: $\Delta\delta^{45}CO_2$ (open circles), $\Delta\delta^{13}$C-CO_2 (filled circles), and $\Delta\delta^{46}CO_2$ (filled diamonds) of BFI tests run by keeping the extracted air sample in the sample trap after extraction and before IRMS analysis for an increasing number of hours (x axis). Δ is defined as the difference between the mean measured and the expected value. Error bars are standard deviations over eight acquisitions during an IRMS analysis. The inset shows how a difference of 1 in $\delta^{46}CO_2$ converts into a difference of 0.035 in δ^{13}C.

increased with increasing time elapsed between extraction and analysis. Tests were run with storage times higher than 24 h to determine the origin of this lag dependence. We inspected the ratios directly reported by the mass spectrometer: $\delta^{45}CO_2$ and $\delta^{46}CO_2$ and found that only the $\delta^{46}CO_2$ was affected by this time dependence (filled diamonds in the lower plot in Figure A1).

[126] Because δ^{13}C and δ^{18}O are calculated from $\delta^{45}CO_2$ and $\delta^{46}CO_2$ (while assuming a known and constant $^{18}O/^{17}O$ ratio) [*Brand et al.*, 2010], a modification of the $\delta^{46}CO_2$, with no corresponding change of the $\delta^{45}CO_2$, also caused a shift of the δ^{13}C (as shown by the filled circles in Figure A1). That change was proportional to the shift in $\delta^{46}CO_2$ (a 1 shift of the measured $\delta^{46}CO_2$ caused a shift of roughly 0.03 of the δ^{13}C, see inset in Figure S1 in the supporting information). If the alteration in the 46/44 ratio were due to contamination with CO_2 produced during extraction, we would expect it to also alter the $\delta^{45}CO_2$. As shown with the open circles in Figure A1, we see no such alteration.

[127] As mentioned in section 2.2.3.1, an influence of the cross contamination on the measured mass 46 could be possible, but its effect should be much smaller than the one described here, especially because the reference of pure CO_2 used in this study had a $\delta^{46}CO_2$ similar to the ones of ice core samples.

[128] In an attempt to identify the cause of the measured $\delta^{46}CO_2$ shift, we ran some numerical simulations. First, we simulated the effect of ethanol at 0.000001% in CO_2 as a contaminant, assuming that it would produce fragments of mass 44 (1%), 45 (50%), and 46 (25%) in the IRMS ion source (http://webbook.nist.gov/cgi/cbook.cgi?ID=C64175&Mask=200#Mass-Spec). We found that the alteration of the 45/44 and 46/44 ratios was not compatible with the observations. We then numerically tested the effect of a nonmass-dependent alteration of the oxygen isotopes ($\Delta r^{17}=\Delta r^{18}$) and found that this is not compatible with the observations either. A nonequilibrium oxygen isotope exchange process, where the trapped CO_2 interacts with residual liquid water present in the sample storage trap, might also be possible. However, we see no reason why it should not alter the measured $\delta^{45}CO_2$. A numerical simulation where only mass 46 is altered can reproduce the observed data (Figure A1), but we could find no physical process consistent with this observation.

A6. Different Types of BFI Tested

[129] To simulate ICELAB extractions, BFI is grown in ICELAB by keeping a container filled with deionized water in thermal equilibrium, in order to grow ice as slowly as possible from the bottom to the top of the container. The container features Plexiglass sidewalls that are electrically heated. The water exchanges heat only through the metallic base and freezes from the bottom to the top. If the process is slow enough, the produced ice is free of visible bubbles.

[130] Bubble-free ice (BFI) used at NIWA (National Institute of Water and Atmospheric research, Wellington, New Zealand, obtained from a supplier for ice sculptures, Southern Ice Distributors Ltd PO Box 38122, Christchurch (H. Schaefer, personal communication, 2010)), as well as BFI produced at the Center for Ice and Climate (University of Copenhagen) were tested, along with the BFI grown in the ICELAB.

[131] Since the different BFIs have been tested by keeping all factors the same, when a higher concentration of one or more measured species is found for only one type of BFI, but not for the others, then the most likely explanation is that the BFI itself is contributing to the enhancement of the measured concentration. Figure A2 shows that there is a strong dependence of the measured offset of CO_2 concentration on the mass of NIWA BFI. The NIWA BFI seems to contain CH_4 too, but not N_2O or CO. The CSIRO BFI might contain N_2O and possibly CO. The CIC (Centre for Ice and Climate) BFI does not show any increase of the concentration of any measured species with the mass of BFI used. However, the average CO_2 offset measured for the CIC BFI is higher than that measured for the CSIRO BFI.

[132] Therefore, we emphasize that bubble-free ice does not necessarily mean gas-free ice. Studies where discrepancies have been found between the expected and measured values when using BFI for extraction tests [*Leuenberger et al.*, 1992; *Lourantou et al.*, 2010] should consider the possibility that the BFI used may actually contain trace amounts of the gas being measured.

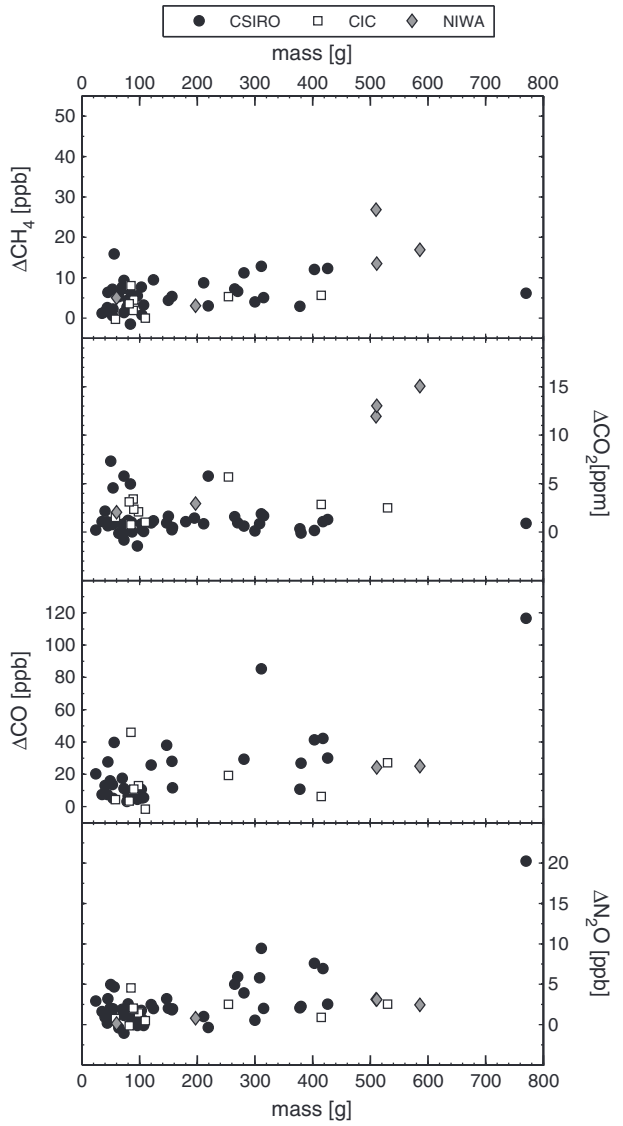

Figure A2. Effect of the BFIs used on the different species: CSIRO- (filled circles), CIC- (open squares) and NIWA- (open diamonds) BFI. Δ is defined as the difference between the mean measured and the expected value.

[133] Although the CSIRO BFI ice performed best for CO_2 and δ^{13}C of the BFIs used here, we still consider possible that a very small amount of gas is trapped in it.

A7. IRMS Sample to Standard Signal Ratio

[134] The mass spectrometer typically compared eight alternating acquisitions of the sample and standard ion ratios to determine average $\delta^{45}CO_2$ and $\delta^{46}CO_2$. To achieve high precision, the signal of the standard is adjusted to closely match that of each sample. While this is relatively easy for typical dual inlet systems measuring sample and standard from bellows, it is more complicated for our system. The MAT252 in GASLAB is equipped with a cryogenic CO_2 extraction accessory (MT Box C, Finnigan) to obtain pure CO_2 out of an air sample. The CO_2 extracted from an air sample is kept in a sample trap at +20 C during measurement. Because the sample is consumed, it provides a signal which is decaying over time. The standard of pure CO_2 is stored in the standard bellows and a small aliquot of this CO_2 is used to provide a standard signal that matches the sample signal, in both initial adjustment and decay rate. The system has been optimized to match initial sample signal of 6 nA (corresponding to 2 V at 3×10^8 , in the cup measuring mass 44 of the MAT252). Large deviations from that signal can lead to bias in the sample to standard signal ratio and, accordingly, to measurement biases. In our system, inaccuracies are considered acceptable in the range 2.5–6.5 V for atmospheric samples, based on analysis of all MAT252 measurements. Since the amount of air extracted from ice cores samples is limited and the precision lower than for atmospheric sample, we decided to accept a minimum threshold of 2 V, which recent tests have indicated delivers acceptable results.

[135] **Acknowledgments.** We thank the following for firn air sampling: the late J.M. Barnola (LGGE) at Law Dome in 1993, T. Sowers (Penn State University) at the South Pole in 1995, A. Smith (ANSTO) and A. Elcheick (Australian Antarctic Division) at Law Dome in 1998, and J. Bastide (Bowdoin University), J. Butler (NOAA), and A. Clarke (NOAA) at South Pole in 2001. S. Coram, R. Gregory, D. Spencer, and D. Thornton provided technical support at CSIRO. Atmospheric samples were provided by staff of the Cape Grim program (supported by the Bureau of Meteorology and CSIRO). South Pole 2001 firn ^{13}C data were provided by INSTAAR, University of Colorado. We thank B. Vaughn for coordinating the data release. The Australian Antarctic Division and the Australian Antarctic Science Program provided long-term ice coring and logistic support in Antarctica. A. Moy, B. Frankel, and M. Nation (Australian Antarctic Division) and Breeze Logistics (Clayton, Victoria) assisted greatly with ice sample handling. We thank Z. Loh and T. Ziehn for comments on the manuscript. This work was undertaken as part of the Australian Climate Change Science Program, funded jointly by the Department of Climate Change and Energy Efficiency, the Bureau of Meteorology, and CSIRO.

References

Allison, C. E., and R. J. Francey (2007), Verifying Southern Hemisphere trends in atmospheric carbon dioxide stable isotopes, *J. Gephys. Res.*, *112*(21), D21304, doi:10.1029/2006JD007345.

Ahn, J., E. J. Brook, L. Mitchell, J. Rosen, J. R. McConnell, K. Taylor, D. Etheridge, and M. Rubino (2012), Atmospheric CO_2 over the last 1000 years: A high-resolution record from the West Antarctic Ice Sheet (WAIS) divide ice core, *Global Biogeochem. Cycles*, *26*(2), GB2027, doi:10.1029/2011GB004247.

Ammann, C. M., F. Joos, D. S. Schimel, B. L. Otto-Bliesner, and R. A. Tomas (2007), Solar influence on climate during the past millennium: Results from transient simulations with the NCAR Climate System Model, presented at the National Academy of Sciences of the United States of America, vol. 104, no. 10, pp. 3713–3718.

Andres, R. J., T. A. Boden, and G. Marland (2011), *Annual Fossil-Fuel CO2 Emissions: Global Stable Carbon Isotopic Signature,* Carbon Dioxide Information Analysis Center, Oak Ridge National Laboratory, U.S. Department of Energy, Oak Ridge Tenn. U.S.A.

Assonov, S. S., C. A. M. Brenninkmeijer, and P. JÃűckel (2005), The ^{18}O isotope exchange rate between firn air CO_2 and the firn matrix at three Antarctic sites, *J. Gephys. Res.*, *110*(18), D18310, doi:10.1029/2005JD005769.

Aydin, M., et al. (2010), Post-coring entrapment of modern air in some shallow ice cores collected near the firn-ice transition: Evidence from CFC-12 measurements in Antarctic firn air and ice cores, *Atmos. Chem. Phys.*, *10*(11), 5135–5144, doi:10.5194/acp-10-5135-2010.

Battle, M., et al. (1996), Atmospheric gas concentrations over the past century measured in air from firn at the South Pole, *Nature*, *383*(6597), 231–235.

Battle, M. O., J. P. Severinghaus, E. D. Sofen, D. Plotkin, E. J. Orsi, M. Aydin, S. A. Montzka, T. Sowers, and P. P. Tans (2011), Controls on the movement and composition of firn air at the West Antarctic Ice Sheet Divide, *Atmos. Chem. Phys.*, *11*(21), 11,007–11,021, doi:10.5194/acp-11-11007-2011.

Beggs, H. M. (1996), Air-sea exchange of CO_2 over the Antarctic seasonal ice zone, PhD thesis, University of Tasmania, Hobart, Tasmania, Australia.

Boden, T. A., G. Marland, and R. J. Andres (2011), *Global, Regional, and National Fossil-Fuel CO_2 Emissions,* Carbon Dioxide Information Analysis Center, Environmental Sciences Division, Oak Ridge National Laboratory, Oak Ridge, Tennessee, U.S.A.

Brand, W. A., S. S. Assonov, and T. B. Coplen (2010), Correction for the ^{17}O interference in (^{13}C) measurements when analysing CO_2 with stable isotope mass spectrometry (IUPAC Technical Report), *Pure Appl. Chem.*, *82*(8), 1719–1733.

Buizert, C., et al. (2012), Gas transport in firn: Multiple-tracer characterisation and model intercomparison for NEEM, Northern Greenland, *Atmos. Chem. Phys.*, *12*(9), 4259–4277, doi:10.5194/acp-12-4259-2012.

Butler, J. H., S. A. Montzka, M. Battle, A. D. Clarke, D. J. Mondeel, J. A. Lind, B. D. Hall, and J. W. Elkins (2001), Collection and analysis of firn air from the South Pole, 2001, Abstract A51F-0145 presented at 2001 Fall Meeting, AGU.

Ciais, P., P. Friedlingstein, D. S. Schimel, and P. P. Tans (1999), A global calculation of the ^{13}C of soil respired carbon: Implications for the biospheric uptake of anthropogenic CO_2, *Global Biogeochem. Cycles*, *13*(2), 519–530.

Conway, T. J., and P. P. Tans (1999), Development of the CO_2 latitude gradient in recent decades, *Global Biogeochem. Cycles*, *13*(4), 821–826.

Cox, P., and C. Jones (2008), Illuminating the modern dance of climate and CO_2, *Science*, *321*(5896), 1642–1644.

Craig, H., Y. Horibe, and T. Sowers (1988), Gravitational separation of gases and isotopes in polar ice caps, *Science*, *242*(4886), 1675–1678.

Elsig, J., J. Schmitt, D. Leuenberger, R. Schneider, M. Eyer, M. Leuenberger, F. Joos, H. Fischer, and T. F. Stocker (2009), Stable isotope constraints on Holocene carbon cycle changes from an Antarctic ice core, *Nature*, *461*(7263), 507–510.

Etheridge, D. M., G. I. Pearman, and F. de Silva (1988), Atmospheric trace-gas variations as revealed by air trapped in an ice core from Law Dome, Antarctica, *Ann. Glaciol.*, *10*, 28–33.

Etheridge, D. M., and C. W. Wookey (1989), Ice core drilling at a high accumulation area of Law Dome, Antarctica, 1987, in *Ice Core Drilling, Proceedings of the Third International Workshop on Ice Core Drilling Technology*, edited by C. Rado and D. Beaudoing, pp. 86–96, CNRS, Grenoble, France.

Etheridge, D. M., L. P. Steele, R. L. Langenfelds, R. J. Francey, J. M. Barnola, and V. I. Morgan (1996), Natural and anthropogenic changes in atmospheric CO_2 over the last 1000 years from air in Antarctic ice and firn, *J. Geophys. Res.*, *101*(D2), 4115–4128.

Etheridge, D. M., L. P. Steele, R. J. Francey, and R. L. Langenfelds (1998), Atmospheric methane between 1000 A.D. and present: Evidence of anthropogenic emissions and climatic variability, *J. Geophys. Res.*, *103*(D13), 15,979–15,993.

Ferretti, D. F., et al. (2006), Atmospheric science: Unexpected changes to the global methane budget over the past 2000 years, *Science*, *309*(5741), 1714–1717.

Francey, R. J., P. P. Tans, C. E. Allison, I. G. Enting, J. W. C. White, and M. Trolier (1995), Changes in oceanic and terrestrial carbon uptake since 1982, *Nature*, *373*, 326–330.

Francey, R. J., L. P. Steele, R. L. Langenfelds, M. Lucarelli, and C. E. Allison (1996), The CSIRO (Australia) measurement of greenhouse gases in the global atmosphere, in *Baseline Atmospheric (Australia) 1999–2000*, edited by N. W. Tindale et al., pp. 42–53, Bureau of Meteorology and CSIRO Division of Atmospheric Research, Melbourne.

Francey, R. J., E. Michel, D. M. Etheridge, C. E. Allison, M. Leuenberger, and D. Raynaud (1997), The pre-industrial difference in CO_2 from Antarctica and Greenland ice, in *Fifth International Carbon Dioxide Conference, Cairns, Australia*, edited by R. Baum et al., pp. 211–212, CSIRO Atmospheric Research, Melbourne, Australia.

Francey, R. J., C. E. Allison, D. M. Etheridge, C. M. Trudinger, I. G. Enting, M. Leuenberger, R. L. Langenfelds, E. Michel, and L. P. Steele (1999), A 1000-year high precision record of ^{13}C in atmospheric CO_2, *Tellus B*, *51*, 170–193.

Francey, R. J., et al. (2013), Atmospheric verification of anthropogenic CO_2 emission trends, *Nat. Clim. Change*, *3*, 520–524, doi:10.1038/nclimate1817.

Frank, D. C., J. Esper, C. C. Raible, U. Büntgen, V. Trouet, B. Stocker, and F. Joos (2010), Ensemble reconstruction constraints on the global carbon cycle sensitivity to climate, *Nature*, *463*(7280), 527–530.

Gerber, S., F. Joos, P. Brügger, T. F. Stocker, M. E. Mann, S. Sitch, and M. Scholze (2003), Constraining temperature variations over the last millennium by comparing simulated and observed atmospheric CO_2, *Clim. Dyn.*, *20*, 281–299.

Goodwin, I. G. (1990), Snow accumulation and surface topography in the katabatic zone of Eastern Wilkes Land, Antarctica, *Antarct. Sci.*, *2*, 235–242.

Gow, A. J. (1965), On the accumulation and seasonal stratification of snow at the South Pole, *J. Glaciol.*, *5*, 467–477.

Houghton, R. A. (2008), *Carbon Flux to the Atmosphere From Land-Use Changes: 1850–2005, A Compendium of Data on Global Change,* Carbon Dioxide Information Analysis Center, Oak Ridge National Laboratory, U.S. Department of Energy, Oak Ridge, Tenn., U.S.A.

Indermühle, A., et al. (1999), Holocene carbon-cycle dynamics based on CO_2 trapped in ice at Taylor Dome, Antarctica, *Nature*, *398*(6723), 121–126.

Joint Committee for Guides in Metrology (2008), Evaluation of measurement data—Guide to the expression of uncertainty in measurement, Bur. Int. des Poids et Mesures Pavillon de Breteuil, France.

Joos, F., M. Bruno, R. Fink, U. Siegenthaler, T. F. Stocker, C. Le Qure, and J. L. Sarmiento (1996), An efficient and accurate representation of complex oceanic and biospheric models of anthropogenic carbon uptake, *Telllus B*, *48*(3), 397–417.

Joos, F., and M. Bruno (1998), Long-term variability of the terrestrial and oceanic carbon sinks and the budgets of the carbon isotopes ^{13}C and ^{14}C, *Global Biogeochem. Cycles*, *12*(2), 277–205.

Joos, F., R. Meyer, M. Bruno, and M. Leuenberger (1999), The variability in the carbon sinks as reconstructed for the last 1000 years, *Geophys. Res. Lett.*, *26*(10), 1437–1440.

Kawamura, K., T. Nakazawa, T. Machida, S. Morinoto, S. Aoki, M. Ishizawa, Y. Fujii, and O. Watanabe (2000), Variations of the carbon isotopic ratio in atmospheric CO_2 over the last 250 years recorded in an ice core from H1S, Antarctica, *Polar Meteorology and Glaciology*, *14*, 47–57.

Keeling, C. D., R. B. Bacastow, A. F. Carter, S. C. Piper, T. P. Whorf, M. Heimann, W. G. Mook, and H. Roellofzen (1989), A three dimensional model of atmospheric CO_2 transport based on atmospheric winds: 1. Analysis of observational data, in *Aspects of Climate Variability in the Pacific and the Western Americas, Geographical Monographs Series, 55*, edited by D H. Peterson, pp.165–236, AGU, Washington D.C.

Köhler, P., H. Fischer, J. Schmitt, and G. Munhoven (2006), On the application and interpretation of Keeling plots in paleoclimate research—Deciphering $^{1}3C$ of atmospheric CO_2 measured in ice cores, *Biogeosciences*, *3*, 539–556.

Krakauer, N. Y., J. T. Randerson, F. W. Primeau, N. Gruber, and D. Menemenlis (2006), Carbon isotope evidence for the latitudinal distribution and wind speed dependence of the air-sea gas transfer velocity, *Tellus*, *58B*, 390–417.

Leuenberger, M., U. Siegenthaler, and C. C. Langway (1992), Carbon isotope composition of atmospheric CO_2 during the last ice age from an Antarctic ice core, *Nature*, *357*(6378), 488–490.

Levchenko, V. A., R. J. Francey, D. M. Etheridge, C. Tuniz, J. Head, V. I. Morgan, E. Lawson, and G. Jacobsen (1996), The ^{14}C "bomb spike" determines the age spread and age of CO_2 in Law Dome firn and ice, *Geophys. Res. Lett.*, *23*(23), 3345–3348.

Lourantou, A., J. V. Lavrič, P. Köhler, J. M. Barnola, D. Paillard, E. Michel, D. Raynaud, and J. Chappellaz (2010), Constraint of the CO_2 rise by new atmospheric carbon isotopic measurements during the last deglaciation, *Global Biogeochem. Cycles*, *24*, GB2015, doi: 10.1029/2009GB003545.

MacFarling Meure, C., D. E. Etheridge, C. Trudinger, P. Steele, R. Langenfelds, T. van Ommen, A. Smith, and J. Elkins (2006), Law Dome CO_2, CH_4 and N_2O ice core records extended to 2000 years BP, *Geophys. Res. Lett.*, *33*(14), L14810, doi:10.1029/2006GL026152.

Machida, T., T. Nakazawa, H. Narita, Y. Fujii, S. Aoki, and O. Watanabe (1996), Variations of the CO_2, CH_4 and N_2O concentration and ^{13}C of CO_2 in the glacial period deduced from an Antarctic ice core, South Yamato, in *Symposium on Polar Meteorology and Glaciology, Proceedings of the National Institute of Polar Research,* vol. 10, edited by O. Watanabe, pp. 55–65.

Mann, M. E., Z. Zhang, M. K. Hughes, R. S. Bradley, S. K. Miller, S. Rutherford, and F. Ni (2008), Proxy-based reconstructions of hemispheric and global surface temperature variations over the past two millennia, *Proceedings of the National Academy of Sciences of the United States of America*, *105*(36), 13,252–13,257.

Masarie, K. A., et al. (2001), NOAA/CSIRO flask air intercomparison experiment: A strategy for directly assessing consistency among atmospheric measurements made by independent laboratories, *J. Geophys. Res.*, *106*(D17), 20,445–20,464.

Mischler, J. A., T. A. Sowers, R. B. Alley, M. Battle, J. R. McConnell, L. Mitchell, T. Popp, E. Sofen, and M. K. Spencer (2009), Carbon and hydrogen isotopic composition of methane over the last 1000 years, *Global Biogeochem. Cycles*, *23*, GB4024, doi:10.1029/2009GB003460.

Mitchell, L. E., E. J. Brook, T. Sowers, J. R. McConnell, and K. Taylor (2011), Multidecadal variability of atmospheric methane, 1000–1800 C.E, *J. Geophys. Res.*, *116*, G02007, doi:10.1029/2010JG001441.

Mook, W. J., J. C. Bommerson, and W. H. Staverman (1974), Carbon isotope fractionation between dissolved bicarbonate and gaseous carbon dioxide, *Earth Planet. Sci. Lett.*, *22*, 169–176.

Morgan, V. I., C. W. Wookey, J. Li, T. D. van Ommen, W. Skinner, and M. F. Fitzpatrick (1997), Site information and initial results from deep ice drilling on Law Dome, Antarctica, *J. Glaciol.*, *43*, 3–10.

Oppo, D. W., Y. Rosenthal, and B. K. Linsley (2009), 2,000-Year-long temperature and hydrology reconstructions from the Indo-Pacific warm pool, *Nature*, *460*(7259), 1113–1116.

Plummer, C. T., M. A. J. Curran, T. D. van Ommen, S. O. Rasmussen, A. D. Moy, T. R. Vance, H. B. Clausen, B. M. Vinther, and P. A. Mayewski (2012), An independently dated 2000-yr volcanic record from Law Dome, East Antarctica, including a new perspective on the dating of the 1450s CE eruption of Kuwae, Vanuatu, *Clim. Past*, *8*, 1929–1940.

Rafelski, L. E., S. C. Piper, and R. F. Keeling (2009), Climate effects on atmospheric carbon dioxide over the last century, *Tellus B*, *61*(5), 718–31.

Randerson, J. T., G. J. Collatz, J. E. Fessenden, A. D. Munoz, C. J. Still, J. A. Berry, I. Y. Fung, N. Suits, and A. S. Denning (2002), A possible global covariance between terrestrial gross primary production and $^{1}3C$ discrimination: Consequences for the atmospheric ^{13}C budget and its response to ENSO, *Global Biogeochem. Cycles*, *16*(4), 83–1, doi:10.1029/2001GB001845.

Scholze, M., J. O. Kaplan, W. Knorr, and M. Heimann (2003), Climate and interannual variability of the atmosphere-biosphere $^{13}CO_2$ flux, *Global Biogeochem. Cycles*, *30*(2), 69–1., doi: 10.1029/2002GL015631.

Scholze, M., P. Ciais, and M. Heimann (2008), Modeling terrestrial ^{13}C cycling: Climate, land use and fire, *Global Biogeochem. Cycles*, *22*(1), GB1009, doi:10.1029/2006GB002899.

Schwander, J., B. Stauffer, and A. Sigg (1988), Air mixing in firn and the age of the air at pore close-off, *Ann. Glaciol.*, *10*, 141–145.

Schwander, J. (1989), The transformation of snow to ice and the occlusion of gases, in *Glaciers and Ice Sheets*, edited by H. Oeschger and C. C Langway Jr., pp. 53–67, Wiley, New York.

Severinghaus, J. P., A. Grachev, and M. Battle (2001), Thermal fractionation of air in polar firn by seasonal temperature gradients, *Geochem. Geophys. Geosyst.*, *2*(7), 1048, doi:10.1029/2000GC000146.

Severinghaus, J. P., and M. Battle (2006), Fractionation of gases in polar ice during bubble close-off: New constraints from firn air Ne, Kr and Xe observations, *Earth Planet. Sci. Lett.*, *244*(1–2), 474–500.

Smith, H. J., H. Fischer, M. Wahlen, D. Mastroianni, and B. Deck (1999), Dual modes of the carbon cycle since the Last Glacial Maximum, *Nature*, *400*(6741), 248–250.

Smith, A. M., V. A. Levchenko, D. M. Etheridge, D. C. Lowe, Q. Hua, C. M. Trudinger, U. Zoppi, and A. Elcheikh (2000), In search of in situ radiocarbon in Law Dome ice and firn, *Nuclear Instruments and Methods in Physics Research B*, *172*(1-4), 610–622.

Sowers, T., M. Bender, and D. Raynaud (1989), Elemental and isotopic composition of occluded O_2 and N_2 in polar ice, *J. Geophys. Res.*, *94*(D4), 5137–5150.

Stocker, B. D., K. Strassmann, and F. Joos (2011), Sensitivity of Holocene atmospheric CO_2 and the modern carbon budget to early human land use: Analyses with a process-based model, *Biogeosciences*, *8*, 69–88.

Sturrock, G. A., D. M. Etheridge, C. M. Trudinger, P. J. Fraser, and A. M. Smith (2002), Atmospheric histories of halocarbons from analysis of Antarctic firn air: Major Montreal Protocol species, *J. Geophys. Res.*, *383*(6597), 231–235, doi:10.1029/2002JD002548.

Sugawara, S., K. Kawamura, S. Aoki, T. Nakazawa, and G. Hashida (2003), Reconstruction of past variations of ^{13}C in atmospheric CO_2 from its vertical distribution observed in the firn at Dome Fuji, Antarctica, *Tellus B*, *55*, 159–169, doi:10.1029/2002JD002545.

Trudinger, C., I. G. Enting, D. M. Etheridge, R. J. Francey, V. A. Levchenko, L. P. Steele, D. Raynaud, and L. Arnaud (1997), Modelling air movement and bubble trapping in firn, *J. Geophys. Res.*, *102*(D6), 6747–6763., doi:10.1029/96JD03382.

Trudinger, C., I. G. Enting, R. J. Francey, D. M. Etheridge, and P. J. Rayner (1999), Long-term variability in the global carbon cycle inferred from a high-precision CO_2 and ^{13}C ice-core record, *Tellus Ser. B: Chemical and Physical Meteorology*, *51*(2), 233–248.

Trudinger, C. M. (2000), The carbon cycle over the last 1000 years inferred from inversion of ice core data, PhD thesis, Available at http://www.cmar.csiro.au/e-print/open/trudinger_2001a0.htm.

Trudinger, C. M., D. Etheridge, P. J. Rayner, I. G. Enting, G. A. Sturrock, and R. L. Langenfelds (2002a), Reconstructing atmospheric histories from measurements of air composition in firn, *J. Geophys. Res.*, *107*(24), 4780, doi:10.1029/2002JD002545.

Trudinger, C. M., I. G. Enting, P. J. Rayner, and R. J. Francey (2002b), Kalman filter analysis of ice core data. 2. Double deconvolution of CO_2 and ^{13}C of CO_2 measurements, *J. Geophys. Res.*, *107*(D20), 4423, doi:10.1029/2001JD001112.

Trudinger, C., I. Enting, D. Etheridge, R. Francey, and P. J. Rayner (2005), The carbon cycle over the past 1000 years inferred from the inversion of ice core data, in *A History of Atmospheric CO_2 and its Effects on Plants, Animals and Ecosystems,* vol. 177, edited by J. R. Elheringer et al., pp. 329–349, Springer, New York.

Trudinger, C. M., I. G. Enting, P. J. Rayner, D. M. Etheridge, C. Buizert, M. Rubino, P. Krummel, and T. Blunier (2013), How well do different tracers constrain the firn diffusivity profile? *Atmos. Chem. Phys.*, *13*, 1485–1510.

Tschumi, J., and B. Stauffer (2000), Reconstructing past atmospheric CO_2 concentration based on ice-core analyses: Open questions due to in situ production of CO_2 in the ice, *J. Glaciol.*, *46*(152), 45–53.

van Ommen, T. D., V. I. Morgan, T. H. Jacka, S. Woon, and A. Elcheikh (1999), Near-surface temperatures in the Dome Summit South (Law Dome, East Antarctica) borehole, *Ann. Glaciol.*, *29*, 141–144.

van Ommen, T. D., V. Morgan, and M. A. J. Curran (2004), Deglacial and Holocene changes in accumulation at Law Dome, *Ann. Glaciol.*, *39*, 359–365.